

# Tree decompositions and social graphs

Aaron B. Adcock \*      Blair D. Sullivan †      Michael W. Mahoney ‡

## Abstract

Recent work has established that large informatics graphs such as social and information networks have non-trivial tree-like structure when viewed at moderate size scales. Here, we present results from the first detailed empirical evaluation of the use of tree decomposition (TD) heuristics for structure identification and extraction in social graphs. Although TDs have historically been used in structural graph theory and scientific computing, we show that—even with existing TD heuristics developed for those very different areas—TD methods can identify interesting structure in a wide range of realistic informatics graphs. Among other things, we show that TD methods can identify structures that correlate strongly with the core-periphery structure of realistic networks, even when using simple greedy heuristics; we show that the peripheral bags of these TDs correlate well with low-conductance communities (when they exist) found using local spectral computations; and we show that several types of large-scale “ground-truth” communities, defined by demographic metadata on the nodes of the network, are well-localized in the large-scale and/or peripheral structures of the TDs. Our detailed empirical results for different TD heuristics on toy and synthetic networks help to establish a baseline to understand better the behavior of the heuristics on more complex real-world networks; and our results here suggest future directions for the development of improved TD heuristics that are more appropriate for improved structure identification in realistic networks.

## 1 Introduction

Understanding the properties of realistic informatics graphs such as large social and information networks and developing algorithmic and statistical tools to analyze such graphs is of continuing interest, and recent work has focused on identifying and exploiting what may be termed tree-like structure in these real-world graphs. Since an undirected graph is a tree if any two vertices are connected by exactly one path, or equivalently if it is connected but has no cycles, real-world graphs are clearly not trees in any naïve sense of the word. For example, realistic social graphs have nonzero clustering coefficient, indicating an abundance of cycles of length three. There are, however, more sophisticated notions that can be used to characterize the manner in which a graph may be viewed as tree-like. These are of interest since, e.g., graphs that are trees have many nice algorithmic and statistical properties, and the hope is that graphs that are tree-like inherit some of these nice properties. In particular,  $\delta$ -hyperbolicity is a notion from geometric group theory that quantifies a way in which a graph is tree-like in terms of its distance or metric properties. Alternatively, tree decompositions (TDs) are tools from structural graph theory that quantify a way in which a graph is tree-like in terms of its cut or partitioning properties.

---

\*Department of Electrical Engineering, Stanford University, Stanford, CA 94305. Email: aadcock@stanford.edu

†Department of Computer Science, North Carolina State University, Raleigh, NC 27695. Email: blair.sullivan@ncsu.edu

‡International Computer Science Institute and Department of Statistics, University of California at Berkeley, Berkeley, CA 94720. Email: mmahoney@stat.berkeley.edu

Although TDs and  $\delta$ -hyperbolicity capture very different ways in which a general graph can be tree-like, recent empirical work (described in more detail below) has shown interesting connections between them. In particular, for realistic social and information networks, these two notions of tree-like-ness capture very similar structural properties, at least when the graphs are viewed at large size scales, and this structure is closely related to what may be termed the nested core-periphery or  $k$ -core structure of these networks. Recent work has also shown that computing  $\delta$ -hyperbolicity exactly is extremely expensive, that hyperbolicity is quite brittle and difficult to work with for realistic social graphs, and that common methods to approximate  $\delta$  provide only a very rough guide to its extremal value and associated graph properties. Motivated by this, as well as by the large body of work in linear algebra and scientific computing on practical methods for computing TDs, in this paper we present results from the first detailed empirical evaluation of the use of TD heuristics for structure identification and extraction in social graphs.

Recall that a TD (defined more precisely below) is a specialized mapping of an arbitrary input graph  $G$  into a graph  $H$  that is a tree, where the vertices of  $G$  are placed overlapping subsets (called bags) associated with the nodes of  $H$ . Quantities such as the treewidth—the size of the bag in  $H$  that contains the largest number of vertices from  $G$ —can be used to characterize how tree-like is  $G$ . Having  $H$  consist of a single bag that contains every vertex from  $G$  is a legitimate but trivial TD (since the width is as large as possible for a graph of the given size), and thus one usually focuses on finding “better” TDs, where better typically means minimizing the width. Unfortunately, the problem of finding the treewidth of  $G$  and of finding an optimal TD of  $G$  are both NP-hard, and thus most effort has focused on developing heuristics, e.g., by constructing the TD iteratively by greedily choosing vertices of  $G$  that minimize quantities such as the degree or fill. Since we are interested in applying TDs on realistic graphs, it is these heuristics (to be described in more detail below) that we will use in this paper.

Our main results consist of applying existing TD heuristics on a carefully-chosen suite of real-world and synthetic social graphs. Our goals are to describe the behavior of these TD heuristics on this class of graph data and to use these TD tools to identify and extract useful structure from these graphs. In particular, (in Section 6) we show the following.

- We first show (in Section 6.1) that TD methods can identify large-scale structures in realistic networks that correlate strongly with the recently-described core-periphery structure of these networks, even when using simple greedy TD heuristics. We do this by relating the global “core-periphery” structure of these networks, as captured using the  $k$ -core decomposition, with what we call the “central-perimeter” structure, which is a measure of the centrality or eccentricity of each bag in the TD. We also describe how small-scale structures such as the internal bag structure of TDs of these networks reflects—depending on the density and other properties of these networks—their clustering coefficient and other related clustering properties of the original networks.
- We next show (in Section 6.2) that the peripheral bags of these TDs correlate well with low-conductance communities/clusters (when they exist) found using local spectral computations, in the sense that these low-conductance (i.e., good-conductance) communities/clusters occupy a small number of peripheral bags in the TDs. In particular, this shows that in graphs for which the so-called Network Community Profile (NCP) Plot is upward-sloping (as, e.g., described in [1], and indicating the presence of good small and absence of good large clusters), the small-scale “dips” in the NCP are localized in clusters that are on a peripheral branch in the TD.
- We finally consider (in Section 6.3) how several types of large-scale “ground-truth” communities/clusters, as defined by demographic metadata on the nodes of the network (and that

are not good-conductance clusters), are localized in the TDs. In particular, we look at two social network graphs consisting of friendship edges between students at a university, we use metadata associated with graduation year and residence hall information, and we show that clusters defined by these metadata are well-localized in the large-scale central and/or small-scale peripheral structures of the TDs.

In all these cases, one significant challenge in applying existing TD heuristics—which have been developed for very different applications in scientific computing and numerical linear algebra—is that it can be difficult to determine whether one is observing a “real” property of the networks or an artifact of the particular TD heuristic that was used to examine the network. Thus, we have applied several existing TD heuristics to a range of toy and synthetic data in order to determine their behavior in idealized settings. (See Section 4 and Section 5, respectively.) The toy data consist of a binary tree, a lattice, a cycle, a clique, and a dense random graph, i.e., graphs for which optimal TDs are known, and they help us understand the behavior of TD heuristics in different idealized settings. The synthetic data consists of Erdős-Renyi and power law random graph models, which help us understand the effect of noise/randomness on the TDs. (Other random graph models exhibit similar properties to these models, when their defining parameters are set to correspondingly sparse values.) For these graphs, we place a particular emphasis on the properties of the TDs as the density parameters (i.e., the connection probability for the Erdős-Renyi graphs and the power law parameter for the power law graphs) are varied from very sparse to extremely sparse, and we are interested in how this relates to the large-scale core-periphery structure.

Our detailed empirical results for different TD heuristics on toy and synthetic networks are important for understanding the behavior of these heuristics on more complex real-world networks; but we note that our results on synthetic and real-world networks also suggest future directions for the development of TD heuristics that are more appropriate for social graph data. That is, existing TD heuristics focus on producing minimum-width TDs, which are of interest in more traditional graph theory and linear algebra applications, but they are not well-optimized for finding structures of interest in social graph applications. Although it is beyond the scope of this paper, the development of TD heuristics that are more appropriate for social graph applications (e.g., understanding how the bag structure of those TDs relates to the output of recently-developed local spectral methods that find good small clusters in large networks) is an important question raised by our empirical results.

The remainder of this paper is organized as follows. In Section 2, we present basic definitions from graph theory, along with a detailed discussion of tree decompositions and the algorithms for their construction. We also provide a brief discussion of other prior related work. Section 3 details the datasets we make use of throughout the paper. The subsequent three sections provide our main empirical results—but although our main results involve applying TDs to real-world graphs, since there has been so little work on using TD heuristics on realistic social graphs, we also consider their use in several idealized settings. In particular, in Section 4, we consider several TD heuristics applied to toy graphs; and in Section 5, we consider TD heuristics applied to synthetic random graphs. Then, in Section 6, we present our main results, where we describe the results of applying TDs to a carefully-chosen suite of real-world social graphs. In Section 7, we prove a theoretical result connecting treewidth and treelength with the (very different) notion of  $\delta$ -hyperbolicity, under an assumption on the length of the longest geodesic cycle in the graph; and in Section 8, we provide a brief discussion of results and conclusion.

## 2 Background and Related Work

In this section, we will review relevant graph theory, tree decompositions ideas, and computational methods, as well as relevant related work.

### 2.1 Preliminaries on Graph Theory

Let  $G = (V, E)$  be a *graph* with vertex set  $V$  and edge set  $E \subseteq V \times V$ . Coming from an applied setting, we often refer to graphs as *networks*, and vertices as *nodes*. We will model social and information networks by undirected graphs, and we note that TDs are themselves graphs (constructed from other input graphs). The *degree* of a vertex  $v$ , denoted  $d(v)$ , is defined as the number of vertices that are adjacent to  $v$  (or the sum of the weights of adjacent edges, if the graph is weighted). The average degree is denoted  $\bar{d}$ . A graph is called *connected* if there exists a path between any two vertices. A graph is called a *tree* if it is connected and has no cycles. A vertex in a tree is called a *leaf* if it has degree 1. A graph  $H = (S, F)$  is a subgraph of  $G$  if  $S \subseteq V, F \subseteq E$ . An *induced subgraph* of  $G$  on a set of vertices  $S \subseteq V$  is the graph  $G[S] := (S, S \times S \cap E)$ . Unless otherwise specified, our analyses will always consider the *giant component*, i.e., the largest connected subgraph of  $G$ .

There are several graph measurements in which we will be interested. The *diameter* of a graph is the maximum distance between any two vertices, and the *eccentricity* of a vertex is the maximum distance between that vertex and all other vertices in the graph. Note that the maximum eccentricity of a graph is equal to the diameter. The *clustering coefficient* of a vertex is the ratio of the number of edges present among its neighbors to the maximum possible number of such edges; when we refer to the clustering coefficient of a network, we use the average of the clustering coefficient of all its vertices.

A *cut* is a partitioning of a network’s vertex set into two pieces. The *volume* of a cut is the sum over vertices in the smaller piece of the number of incident edges, while the *surface area* of a cut is the number of edges with one end-point in each piece; in this case, the *conductance* of a cut—one of the most important measures for assessing the quality of a cut—is the surface area divided by the volume (that is, we will be following the conventions used in previous work [1, 2]).

Finally, throughout this paper, we will refer to the “core-periphery” structure of a network. Following prior work (e.g., [1, 3, 2], we use the *k-core decomposition* to identify these core nodes. In particular, the *k*-core of a network  $G$  is the maximal induced subgraph  $H \subseteq G$  such that every node in  $H$  has degree at least  $k$ . The *k*-core has the advantage of being easily computable in  $O(V + E)$  time [4, 5, 6].

### 2.2 Preliminaries on Tree Decompositions

Tree decompositions (TDs) are combinatorial objects that describe specialized mappings of cuts in a network to nodes of a tree. Although they were originally introduced in the context of structural graph theory (specifically, in the proof of the Graph Minors Theorem [7]), TDs have gained significant attention in the broader community due to their use in efficient algorithms for certain NP-hard problems. In particular, there are polynomial-time algorithms for solving many such problems on all graphs that have TDs whose width (defined below) is bounded from above by a constant [8, 9]. These algorithms have been applied to problems in constraint satisfaction (e.g., sensor placement), computational biology, linear algebra, probabilistic networks, and machine learning [10, 11, 12, 13, 14, 15, 16, 17, 18].

**Definition 1.** A tree decomposition (TD) of a graph  $G = (V, E)$  is a pair

$$(X = \{X_i : i \in I\}, T = (I, F)) ,$$

with each  $X_i \subseteq V$ , and  $T$  a tree with the following properties:

1.  $\cup_{i \in I} X_i = V$ ,
2. For all  $(v, w) \in E, \exists i \in I$  with  $v, w \in X_i$ , and
3. For all  $v \in V$ ,  $\{i \in I : v \in X_i\}$  forms a connected subtree of  $T$ .

The  $X_i$  are called the bags of the tree decomposition.

The third condition of the definition is a continuity requirement that allows the TD to be used in dynamic programming algorithms for many NP-hard problems.<sup>1</sup> It is equivalent to requiring that for all  $i, j, k \in I$ , if  $j$  is on the path from  $i$  to  $k$  in  $T$ , then  $X_i \cap X_k \subseteq X_j$ .<sup>2</sup> The quality of a tree decomposition is often measured in terms of its largest bag size:

**Definition 2.** Let  $\mathcal{T} = (\{X_i\}, T = (I, F))$  be a tree decomposition of a graph  $G$ . The width of  $\mathcal{T}$  is defined to be  $\max_{i \in I} |X_i| - 1$ , and the treewidth of  $G$ , denoted  $\text{tw}(G)$ , is the minimum width over all valid tree decompositions of  $G$ . A tree decomposition whose width is equal to the treewidth is often referred to as optimal.

By this definition, trees have the minimum possible treewidth of 1 (their bags contain the edges of the original tree and thus have size 2); but, in contrast to  $\delta$ -hyperbolicity (see Section 2.4), an  $n$ -vertex clique is now the least tree-like graph (attaining the maximum treewidth of  $n - 1$ ). In fact, the only valid TDs of a clique have all vertices in a single bag. Since TDs remain valid under taking subgraphs (once you delete any vertices no longer present), it is straightforward to prove that if  $W$  is any complete subgraph of  $G$ , every TD of  $G$  has some bag that contains all the vertices of  $W$  [19].

Two other canonical examples (to which we will return in detail below) are the cycle and the grid, which have vastly differing treewidths. All cycles (regardless of the number of vertices) have treewidth 2 (see Figure 5 below). The  $n \times n$  planar grid, on the other hand, has treewidth  $n$ , and thus it is not tree-like by this measure. Grids are particularly noteworthy in the discussion of TDs due to a result (described in more detail below) showing that they are essentially the only obstruction to having bounded treewidth.<sup>3</sup>

Finding a TD for a given graph whose width is minimal (equal to the treewidth) is itself an NP-hard problem [21, 12]. We note that most methods (including all those discussed here) for constructing TDs were designed with the goal of minimizing width, as most prior work focused on using these structures to reduce computational cost for an algorithm/application.<sup>4</sup> Also, although treewidth is a graph invariant, TDs of a network are not unique, even under the condition of having

---

<sup>1</sup>Alternatively, the bags and edges of the TD form separators (cuts) in the graph. The set of vertices contained in any bag, or intersection of two adjacent bags, form a separator in  $G$ . This structural property is important as it allows TDs to be thought of as a method of organizing cuts in a network. This is also related to how the treewidth of a network is used to measure how tree-like a network is. Intuitively, a tree has a treewidth of 1 because the graph can be separated by the removal of a single edge (or vertex) in the network, whereas a cycle requires two edges to be cut and thus has a treewidth of 2. TDs with large widths require larger numbers of vertices to separate a network into two disconnected pieces.

<sup>2</sup>In addition, a related aspect of the definition of a TD to be aware of is the overlapping nature of the bags of a TD. Vertices in the graph will appear in many bags in the TD. As shown in previous work [3], this is particularly true of high degree or high  $k$ -core nodes.

<sup>3</sup>In particular, in the so-called Grid Minor Theorem, Robertson and Seymour showed that every graph of treewidth at least  $k$  contains a  $f(k) \times f(k)$  grid as a graph minor, for some integer-valued function  $f$ . The original estimate of the function  $f$  gave an exponential relationship between the treewidth and the grid size, and although several results greatly improved the relationship, the question of whether or not it held for any polynomial function  $f$  remained open for over 25 years. Recently, Chekuri and Chuzhoy proved that there is a universal constant  $\delta > 0$  so that all graphs of treewidth at least  $k$  have a grid-minor of size  $\Omega(k^\delta) \times \Omega(k^\delta)$  [20], resolving this conjecture.

<sup>4</sup>In the context of understanding the intermediate-scale structure of real networks and improving inference (e.g., link prediction, overlapping community detection, etc), there are likely more appropriate objective functions, although their general identification and development is left as future work.

minimum width. For example, see Figure 5 below, which shows several distinct minimum width TDs of a cycle.

Finally, although it is not standard, we will abuse the term *width* to apply it directly to a bag of a tree decomposition (in which case, it takes the value of the cardinality of the set minus one), so that we can talk about the *maximum width* (which is the equivalent to the usual definition of width), and *median width* of a decomposition (which is the median of the widths of the bags).

Further, we will use the term *center* to refer to the bag (or bags) associated with the node(s) of minimum eccentricity in the tree underlying a TD, and the term *perimeter* for bags associated with nodes of relatively high eccentricity. We do this to help provide a framework for discussing the connection in many social and information networks between the core (resp. periphery) of the network and the central (resp. perimeter) bags of its TD computed with certain heuristics. Note that by definition, a tree will have at most two bags at its center.

## 2.3 Constructing Tree Decompositions

Here, we give a brief overview of existing algorithms for constructing TDs; more comprehensive surveys can be found in [12, 22]. The algorithms for finding low-width TDs are generally divided into two classes: “theoretical” and “computational.” The former category includes, for example, the linear algorithm of Bodlaender [23], which checks if a TD of width at most  $k$  exists (for a fixed constant  $k$ ), and the approximation algorithms of Amir [24]. These are generally considered (practically) computationally intractable due to very large hidden constants and complexity of implementation—e.g., Bodlaender’s algorithm was shown by Röhrig [25] to have too high a computational cost even when  $k = 4$ . The approximation algorithms of Amir have been tested on graphs with up to several hundred vertices, but they require hours of running time even at this size scale. There has also been work on exact algorithms, the most computational of which is perhaps the QuickTree algorithm of Shoikhet and Geiger, which was tested on graphs with up to about 100 vertices and treewidth 11 [26].

Thus, in practice, most computational work requires the use of heuristic approaches (i.e., those which offer no worst-case guarantee on their maximum deviation from optimality). Since we are interested in applying TDs to real network data, we will focus on these “practical” algorithms in the remainder of this paper. For the reader interested in experimenting with implementations of some of these algorithms, this work uses the routines in INDDGO [27, 28], an open source software suite for computing TDs and numerous graph and TD parameters.

### 2.3.1 Chordal Graph Decomposition

One of the most common methods for constructing TDs is based on known algorithms for decomposing *chordal graphs*. Thus, we start with the following definition.

**Definition 3.** *A graph  $G$  is chordal if it has no induced cycles of length greater than three (equivalently, every cycle in  $G$  with length at least four, has a chord).*

Equivalently, chordal graphs are characterized by the existence of an ordering  $\pi = (v_1, \dots, v_n)$  of their vertices so that for each  $v_i$ , the set of its neighbors  $v_j$  with  $j > i$  form a clique. This ordering is called a *perfect elimination ordering*, and it gives a straightforward construction for a TD (also called the clique-tree) of a chordal graph, with bags consisting of the sets of higher-indexed neighbors of each vertex.

For a general graph  $G$ , one common approach for finding TDs is to first find a chordal graph  $H$  containing  $G$ , then use the associated TD (since as we mentioned earlier, TDs remain valid for all subgraphs on the same vertex set. The typical approach is via *triangulation*, a process that

uses a permutation of the vertex set (called the *elimination ordering*) to guide the addition of edges, which are referred to as *fill* edges. Note that chordal completions are certainly not unique. For example, the complete graph formed on the vertices of  $G$  is chordal and contains  $G$ ; although, in some sense, it is a trivial or the “worst” triangulation (in the sense that it has the most fill edges and largest possible clique subgraph among all triangulations).

We will use the notation  $G_\pi^+$  to denote the triangulation of  $G$  using ordering  $\pi$ , and an outline of the process is given in Algorithm 1. The process for finding a TD  $T_\pi$  using an elimination order  $\pi$  and Gavril’s algorithm ([29]) for decomposing chordal graphs is given in Algorithm 2. Note that we may refer to the *width* of an ordering, by which we mean the treewidth of the chordal graph  $G_\pi^+$ . The literature includes several slight variants on Gavril’s construction routine (such as Algorithm 2 in [22]), but the overall process and width of the TD produced is the same for each.

---

**Algorithm 1** Triangulate a graph  $G$  into a chordal graph  $G_\pi^+$ 


---

INPUT: Graph  $G = (V, E)$ , and  
 $\pi = (v_1, \dots, v_n)$ , a permutation of  $V$   
OUTPUT: Chordal graph  $G_\pi^+ \supseteq G$ , for which  
 $\pi$  is a perfect elimination ordering

- 1: Initialize  $G_\pi^+ = (V', E')$  with  $V' = V$  and  $E' = E$
- 2: **for**  $i = 1$  to  $n$  **do**
- 3:     Let  $N_i = \{v_j \mid j > i \text{ and } (v_i, v_j) \in E\}$
- 4:     **for**  $\{x, y\} \subseteq N_i$  **do**
- 5:         **if**  $x \neq y$  and  $(x, y) \notin N_i$  **then**
- 6:              $E' = E' \cup \{(x, y)\}$
- 7:         **end if**
- 8:     **end for**
- 9: **end for**
- 10: **return**  $G_\pi^+$

---

Perhaps surprisingly, there is always some elimination ordering which produces an optimal TD (one of minimum width), and this may co-occur with high fill. The following theorem (a proof of which may be found in [22]) presents the connections between treewidth, triangulations, and elimination orderings.

**Theorem 1.** *Let  $G = (V, E)$  be a graph, and let  $k \leq n$  be a non-negative integer. Then the following are equivalent.*

1.  *$G$  has treewidth at most  $k$ .*
2.  *$G$  has a triangulation  $H$  such that any complete subgraph of  $H$  (clique) has at most  $k + 1$  vertices.*
3. *There is an elimination ordering  $\pi$ , such that  $G_\pi^+$  does not contain any clique on  $k + 2$  vertices as a subgraph.*
4. *There is an elimination ordering  $\pi$ , such that no vertex  $v \in V$  has more than  $k$  neighbors in  $G_\pi^+$  which occur later in  $\pi$ .*

Thus, if one can produce a “good” elimination ordering of a graph (meaning one with a small maximum clique), it is easy to construct a low-width TD of the graph, and such an ordering always exists if the treewidth is bounded. The intuition behind using fill-reducing orderings to minimize width follows from the idea that in order to produce a large clique that wasn’t already in the network, one “should” have to add many fill edges.

---

**Algorithm 2** Construct a tree decomposition  $T_\pi$  of a graph  $G$  using elimination ordering  $\pi$  and Gavril’s algorithm

---

INPUT: Graph  $G = (V, E)$ ,  $\pi$  a permutation of  $V$   
 OUTPUT: Tree decomposition  $T_\pi = (X, (I, F))$  with  
 $(I, F)$  a tree, and bags  $X = \{X_i\}$ ,  $X_i \subseteq V$

- 1: Initialize  $T = (X, (I, F))$  with  $X = I = F = \emptyset$ ,  $n = |V|$
- 2: Create an empty  $n$ -long array  $t[]$
- 3: ELIMINATE using  $\pi$  to create triangulation  $G_\pi^+$
- 4: Let  $k = 1$ ,  $I = \{1\}$ ,  $X_1 = \{\pi_n\}$ ,  $t[\pi_n] = 1$
- 5: **for**  $i = n - 1$  to 1 **do**
- 6:     Find  $B_i = \{\text{neighbors of } \pi_i \text{ in } G_\pi^+\} \cap \{\pi_{i+1}, \dots, \pi_n\}$
- 7:     Find  $m = j$  such that  $j \leq k$  for all  $\pi_k \in B_i$
- 8:     **if**  $B_i = X_{t[m]}$  **then**
- 9:          $X_{t[m]} = X_{t[m]} \cup \{\pi_i\}$ ;  $t[\pi_i] = t[m]$
- 10:     **else**
- 11:          $k = k + 1$
- 12:          $I = I \cup \{k\}$ ;  $X_k = B_i \cup \{\pi_i\}$
- 13:          $F = F \cup \{(k, t[m])\}$ ;  $t[\pi_i] = k$
- 14:     **end if**
- 15: **end for**
- 16: **return**  $T_\pi = (X, (I, F))$

---

### 2.3.2 Ordering Heuristics

In this section, we describe the landscape of heuristics for creating elimination orderings, focusing on those subsequently tested in our empirical evaluations. For the reader interested a more detailed analysis of each heuristic as well as the theoretical connections between chordal graphs and TD, see [22] and the original references included throughout this section.

Unfortunately, the space of all possible elimination orderings is  $O(n!)$  for a graph on  $n$  vertices, making it impractical to search using brute force techniques. One possibility for exploring the space is to apply a stochastic local search approach like simulated annealing, which often finds a good solution after sufficiently many iterations; but since this is relatively slow, it is not commonly seen in practice.

The first class of specialized methods are known as triangulation recognition heuristics, and include lexicographic breadth-first-search (LEX-M) and maximum cardinality search (MCS) [22, 30, 31, 32, 33, 34, 35]. These methods are guaranteed to provide a perfect elimination ordering for chordal graphs, so many believed they would produce low-fill and/or low-width orderings for more general graphs. In [22], the authors report good results with respect to width when using these methods on graphs which are already chordal or have regular structures, but poor results compared to the greedy heuristics when even small amounts of randomness is added to the network. Further empirical evaluation in [27] supports these claims; additionally, these heuristics are too computationally expensive to run on very large graphs.

A large set of additional heuristics uses the idea of splitting the graph (using a small separator), recursively decomposing the resulting pieces, and then “gluing” the solutions into a single TD (this includes [24, 36, 37, 38, 11, 39] and many others). To quote Bodlaender and Koster [22], “they are significantly more complex, significantly slower, and often give bounds that are higher than those of simple algorithms,” and so we refer the interested reader to their survey for additional details and references. We do, however, use a related approach that finds a set of nested graph partitions,

but instead of decomposing the resulting pieces, it places the separators into an elimination ordering. This approach is called *nested dissection* [40, 41] and it is quite popular for computing fill-reducing orderings for sparse matrices in numerical linear algebra. The algorithm recursively finds a small vertex separator (bisector) in a graph, and it ensures that in the resulting elimination ordering, the vertices in the two components formed by the bisection all appear before the vertices in the separator. We use the “node nested dissection” algorithm implemented in METIS [42] (called through INDDGO), and thus we refer to this heuristic as METNND. In METIS, the recursion is stopped when the components are smaller than a certain size, and some version of minimum degree ordering is then applied to the remaining pieces. The software “grows” each bisection using a greedy node-based strategy. It is worth noting that since it is searching for bisections, there is a tunable “balance” condition (determining how close to 50/50 the split needs to be), although for all computations reported in this paper, we left the parameter at its default value.

Finally, the perhaps most popular class of elimination ordering routines are the so-called *greedy* heuristics, named because they make greedy decisions to pick the subsequent node in the elimination ordering. There are innumerable variations, but the most common are based around two basic concepts: choosing a vertex to minimize *fill* (how many new edges will be added to the graph if a vertex is chosen to be next in the ordering); or choosing a vertex of minimum degree (low-degree vertices have small neighborhoods, which also limits the potential fill). When applied in their most rudimentary forms, these are called the MINDEG [43] and MINFILL orderings. Both of these strategies indirectly limit the size of cliques produced in the final triangulation (although they were originally designed to minimize the number of fill edges added during the triangulation, a quantity which is not always correlated). For additional heuristics combining these strategies and incorporating additional local information, see [22].

Even though keeping updated vertex degrees for MINDEG during triangulation (greedy orderings make their decisions based on a partially triangulated graph at each step) is significantly less computationally intensive than computing current vertex fills for MINFILL, there have been important efforts to further reduce the complexity. In particular, we note the approximate minimum degree or AMD heuristic [44, 45]. This heuristic computes an upper bound on the degree of each node in each pass using techniques based on the quotient graph for matrix factorization, and it has been shown to be significantly faster and of similar quality (in terms of fill and width minimization). We use AMD interchangeably with the traditional MINDEG, especially on larger networks.

## 2.4 Additional Related Work

For completeness, we provide here a brief overview of the large body of additional related work. As already mentioned, TDs played an important role in the proving of the graph minor theorem [7], but they have also become popular in theoretical computer science, as many NP-hard optimization problems have a polynomial time algorithm for graphs with bounded treewidth [8]. In addition, bounding the treewidth of the underlying graph of probabilistic graphical models allows for fast inference computations [46].

Additional overviews of TDs and their uses in discrete optimization are available [47, 48, 49, 50]; and one can also learn more about the uses of these methods in numerical linear algebra and sparse matrix computations [51], as well as connections with triangulation methods: triangulation of minimum treewidth [52], empirical work on treewidth computations [53], the minimum degree heuristic and connections with triangulation [54], and a survey of triangulation methods [55]. In addition, the treewidth of random graphs for various parameter settings has been studied [56, 57].

A different notion of tree-like-ness is provided by  $\delta$ -hyperbolicity; early more mathematical

work did not consider graphs and networks [58, 59], but more recent more applied work has [60, 61, 62]. Computing  $\delta$  exactly is very expensive [63], and sampling-based methods to approximate it provide only a very rough guide to its value and properties [3]. For many references on  $\delta$ -hyperbolicity in network analysis, see [62] (and the more recent paper [64]) and references therein. In addition, there has been work on trying to relate hyperbolicity and TD-based ideas, often going beyond treewidth to consider other metrics such as treelength or chordality or the expansion properties of the graph; see, e.g., [65, 66, 67, 68, 69, 70, 71, 72, 73].

Recent work in network analysis and community structure analysis has pointed to some sort of “core-periphery” structure in many real networks [1, 74, 75, 3, 2]; and recently this has been related to the  $k$ -core decomposition—see, e.g., [3] and references therein. The  $k$ -core decomposition is of interest more generally, and additional references for  $k$ -core decompositions, including their use in visualization and in larger-scale applications, include [76, 77, 78, 79, 80, 81, 82]. Questions of well-connected or expander-like cores are of particular interest in applications having to do with diffusion processes, influential spreaders, and related questions of social contagion [83, 84].

There are a few papers that have used TDs to investigate the structural properties of social and information networks: e.g., to look at the tree-like-ness of internet latency and bandwidth [85]; to compare hyperbolicity and treewidth on internet networks [86]; and to examine the relationship between hyperbolicity, treewidth, and the core-periphery structure in a much wider range of social and information networks [3]. In particular, [86] concludes that the hyperbolicity is small in the networks they examined but the treewidth is relatively large, presumably due to a highly connected core; and [3] concludes that many real social and information networks do have a tree-like structure, with respect to both metric-based hyperbolicity and (in spite of the large treewidth) the cut-based TDs, that corresponds to the core-periphery structure of the network. Finally, very recently we became aware of [87].

### 3 Network Datasets

We have examined the empirical performance of existing TD heuristics on a broad set of real-world social and information networks as well as a large corpus of synthetic graphs. The real-world networks have been chosen to be representative of a broad range of networks, as analyzed in prior work [1, 3, 2], and the synthetic graphs have been chosen to illustrate the behavior of TD methods in relatively controlled settings. See Table 1 for a summary of the networks we have considered. Note that the real-world graphs are connected, but we are interested in parameter values for the synthetic graphs which might cause the instances to be *disconnected*. In these cases, we work with the giant component, and the statistics that are shown in Table 1 are for this connected subgraph.

**Erdős-Rényi (ER) graphs.** Although ER graphs are often criticized for their inability to model pertinent properties of realistic networks, *extremely* sparse ER graphs have several structural inhomogeneities that will be important for understanding tree-like structure in realistic networks [3].<sup>5</sup> In particular, recall that, in the extremely sparse regime of  $1/n < p < \log(n)/n$ , ER graphs are (w.h.p.) not even fully connected; ER graphs in this regime have an upward-trending NCP (network community profile) [1]; with respect to their  $k$ -core structure, a shallow (but non-trivial) core-periphery structure emerges [3, 88]; and with respect to their metric properties (as measured with  $\delta$ -hyperbolicity), graphs in this regime have nontrivial tree-like properties [3]. Following previous work [3], we set the target number of vertices to  $n = 5000$ , and we choose  $p = \frac{d}{n}$  for various values of  $d$  from  $d = 1.6$  to  $d = 32$ . We denote these networks using  $\text{ER}(d)$ .

---

<sup>5</sup>The same is true for many other less unrealistic random graph models, assuming their parameters are set to analogously sparse values.

Network	$n_c$	$k_l$	$k_m$	$\bar{d}$	$\bar{C}$	$D$
ER Random Graphs						
ER(1.6)	3210	1	2	2.16	0.00	38
ER(1.8)	3617	1	2	2.28	$9.30 \times 10^{-4}$	34
ER(2)	4001	1	2	2.39	$9.11 \times 10^{-4}$	30
ER(4)	4879	1	3	4.05	$8.96 \times 10^{-3}$	15
ER(8)	4998	1	5	8.04	$1.59 \times 10^{-3}$	7
ER(16)	5000	4	11	16.1	$3.13 \times 10^{-3}$	5
ER(32)	5000	7	23	32.1	$6.39 \times 10^{-3}$	4
PL Random Graphs						
PL(2.50)	4895	1	4	2.78	$2.46 \times 10^{-3}$	18
PL(2.75)	4650	1	2	2.43	$6.99 \times 10^{-4}$	22
PL(3.00)	4071	1	2	2.24	$1.18 \times 10^{-3}$	29
SNAP Social Graphs						
CA-GRQC	4158	1	43	6.46	.665	17
CA-ASTROPH	17903	1	56	22.0	.669	14
AS20000102	6474	1	12	3.88	.399	9
GNUTELLA09	8104	1	10	6.42	.0137	10
EMAIL-ENRON	33696	1	43	10.7	.708	13
FB Social Graphs						
FB-CALTECH	762	1	35	43.7	.426	6
FB-HAVERFORD	1446	1	63	82.4	.327	6
FB-LEHIGH	5073	1	62	78.2	.270	6
FB-RICE	4083	1	72	90.5	.300	6
FB-STANFORD	11586	1	91	98.1	.252	9
Miscellaneous Graphs						
POWERGRID	4941	1	5	2.67	0.107	46
POLBLOGS	1222	1	36	27.4	0.360	8
PLANARGRID	2500	2	2	3.92	0.00	98
ROAD-TX	1379917	1	3	1.39	0.0209	1054
WEB-STANFORD	281903	1	71	8.20	$2.89 \times 10^{-3}$	674

Table 1: Statistics of analyzed networks: nodes in giant component  $n_c$ ;  $k_l$  the lowest  $k$ -core;  $k_m$  the maximum  $k$ -core; average degree  $\bar{d} = 2E/N$ ; average clustering coefficient  $\bar{C}$ ; and diameter  $D$ .

Table 1 clearly shows that, as a function of *increasing*  $d$ , i.e., increasing  $p$ , the size of the giant component increases to 5000, the number of edges increases dramatically, the clustering coefficient remains close to zero, the average degree  $\bar{d}$  increases, and the diameter decreases dramatically.

**Power Law (PL) graphs.** We also considered the Chung-Lu model [89], an ER-like random graph model parameterized to have a power law degree distribution (in expectation) with power law (or heterogeneity) parameter  $\gamma$ , which we vary between 2 and 3. We denote these networks using  $PL(\gamma)$ . We consider values of the degree heterogeneity parameter  $\gamma \in \{2.50, 2.75, 3.00\}$ . Table 1 shows that, as a function of *decreasing*  $\gamma$ , the size of the giant component increases, the average degree  $\bar{d}$  increases, and the diameter decreases. Although not shown in Table 1, as  $\gamma$  decreases, PL graphs also form a rather prominent, and moderately-deep,  $k$ -core structure [3]. These are all trends that parallel the behavior of ER as  $d$  increases.<sup>6</sup>

**SNAP graphs.** We selected various social/information networks that were used in the large-scale empirical analysis that first established the upward-sloping NCP and associated nested core-periphery for a broad range of realistic social and information graphs [1]. These are avail-

<sup>6</sup>For sparse ER graphs, this happens since there is not enough edges for concentration of measure to occur, i.e., for empirical quantities such as the empirical degrees to be very close to their expected value. For PL graphs, an analogous lack of measure concentration occurs due to the exogenously-specified heterogeneity parameter  $\gamma$ .

able at the SNAP website [90]. In particular, the networks we considered are CA-GRQC and CA-ASTROPH (two collaboration networks); AS20000102 (an autonomous system snapshot); GNUTELLA09 (a peer-to-peer network from Gnutella); EMAIL-ENRON (an email network from the Enron database); as well as the Stanford Web network WEB-STANFORD and the Texas road network ROAD-TX. These networks are very sparse, e.g., fewer than ca. 10 edges per node; and they exhibit substantial degree heterogeneity, moderately high clustering coefficients (except for GNUTELLA09, WEB-STANFORD, and ROAD-TX), and moderately small diameters. In addition, although not presented in Table 1 (and with the exception of ROAD-TX), these graphs have a much stronger core-periphery structure, as measured by the  $k$ -core decomposition, than typical synthetic networks [3, 2, 1].

**Facebook Networks.** We selected several representative Facebook graphs out of ca. 100 Facebook graphs from various American universities collected in ca. 2005 [91]. These data sets range in size from around 700 vertices (FB-CALTECH) to approximately 30,000 vertices (FB-TEXAS84). In particular, we examine FB-CALTECH, FB-RICE, FB-HAVERFORD, FB-LEHIGH, and FB-STANFORD in this paper. These networks all arise via similar generative procedures, and thus not surprisingly there are strong similarities between them. There are a few distinctive networks, however, that are worth mentioning. In particular, several universities (FB-CALTECH, FB-RICE, FB-UCSC) have a particularly strong resident housing system, and it is known that this manifests itself in structural properties of the graphs [91]. Below, we will use the meta-information associated with this housing system to provide “ground-truth” clusters/communities for comparison and evaluation.<sup>7</sup> One important characteristic to observe from Table 1 is that these Facebook networks, while sparse, are much denser than any of the SNAP graphs we consider or that were considered previously [1].<sup>8</sup>

**Miscellaneous Networks.** We also selected a variety of real-world networks that, based on prior work [1, 3, 2], are known to have very different properties than the SNAP social graphs or the Facebook social graphs. In particular, we consider POLBLOGS, a political bloggers network [92] (a graph constructed from political blogs which are linked); the Western US power grid POWERGRID [93]; and a two-dimensional  $50 \times 50$  planar grid PLANARGRID.

## 4 Tree decompositions of toy networks

Before proceeding with the synthetic and real-world data, in this section we will describe the results of using a variety of TD heuristics on a set of very simple “toy” networks, on which the optimal-width TDs are known. The five toy networks we consider are a binary tree (SMALLBINARY), a small section of the two-dimensional planar grid (SMALLPLANAR), a cycle (SMALLCYCLE), a clique (SMALLCLIQUE), and an Erdős-Rényi graph with an edge probability of  $p = 0.5$  (SMALLER). Each of these networks has 100 nodes (except for SMALLCYCLE, which has only 10 nodes—the reason for this is that the principal change by having a larger cycle is that the eccentricity of the decompositions becomes much larger, which simply makes it more difficult to visualize—and SMALLBINARY, which has 128 nodes to maintain symmetry). In Figure 1, we provide visualizations of each of the five networks. (These visualizations were created with the GraphViz command *neato* [94], which was used for all network visualizations in this paper, and with the help of [95, 96].)

We begin with these very simple network topologies to illustrate the behavior of different TD

---

<sup>7</sup>See [2] for how this affects the NCP of these networks.

<sup>8</sup>Among the differences caused by the much higher density of Facebook networks is that these networks have a much deeper  $k$ -core structure than the other real networks, and they tend to lack deep cuts, e.g., they lack even good very-imbalanced partitions such as those responsible for the upward-sloping NCP [1, 2].

heuristics in a range of very simple and controlled settings. For example, while **SMALLBINARY** is a tree, the other graphs are not; the two-dimensional grid is quite different from a tree, as is **SMALLCYCLE** (although, from the treewidth perspective it is fairly close to a tree), and both have high-quality well-balanced partitions; and both **SMALLCLIQUE** and **SMALLER** are expanders (not constant degree expanders, but expanders in the sense that they don't have any good partitions) and thus very non-tree-like (from the TD perspective), but each has important differences with respect to their respective TDs. Among other things, we will focus on which types of structures different heuristics tend to capture, as well as how different heuristics deal with nodes (not bags) which are associated with the core or periphery of the original network. Importantly, these toy networks have basic constructions, and they (mostly) have known optimal width TDs—e.g., **SMALLPLANAR** and **SMALLCYCLE** have several known equivalent minimum width TDs—and the **SMALLER** network serves to illustrate some of the effects of randomness on a TD. Although a TD is a complex object, we will see that the insights we obtain here can be used to interpret the output of TD heuristics in much more complex synthetic and real networks.

#### 4.1 TD properties of toy networks

In Figures 2, 3, and 4, we show visualizations of TDs produced by various heuristics (the greedy **MINDEG** in Figure 2; the **METNND**, nested node dissection via **METIS**, in Figure 3; and **LEXM** in Figure 4) for each of these five toy networks. In these visualizations, the size of the bag corresponds with the bag's width, and the coloring is based on the fraction of edges present in the induced subgraph of the bag. In particular, if the nodes in the bag form a clique in the original network, then the fraction of edges present is 1.0 and the bag would be colored dark red; while if the the nodes are completely disconnected in the original network, then the bag will be colored dark blue.

From these figures, we see that there are substantial differences between the TDs that different heuristics generate for these five toy networks. All the heuristics give the same uninteresting results for **SMALLCLIQUE**; but for all of the other networks, including **SMALLBINARY**, we observe that there are differences in the decompositions produced by the different heuristics. The most illuminating of these differences are seen in **SMALLPLANAR**, **SMALLCYCLE**, and **SMALLER**. For both **SMALLPLANAR** and **SMALLER**, **MINDEG** and **METNND** return TDs with several prominent branches, while **LEXM** returns a path for the TD. For **MINDEG**, this is due to the tendency of the algorithm to pick low-degree nodes on the “outside” of the network and then work its way around the outside of the network. For **METNND**, this is due to the tendency of the algorithm to cut the networks repeatedly into smaller pieces and then recursively “eat away” at these smaller pieces to form the TD. On the other hand, the **LEXM** heuristic works to produce a minimal triangulation using lexicographic labelings along paths. In many realistic networks, and in particular in **SMALLPLANAR** and **SMALLER**, this results in a path-like TD, as the algorithm uses a breadth-first search through the network. On the other hand, for **SMALLCYCLE**, **METNND** returns a branchy TD, while both **MINDEG** and **LEXM** return path TDs.

In Tables 2 and 3, we provide basic statistics for TD heuristics applied to each of these networks. In particular, Table 2 shows a summary of our results for the the (maximum) width of TDs produced by various heuristics (for **SMALLER**, the width given is averaged and rounded over five different instantiations of the network). We ignore the issue of tie-breaker choices (e.g., in **MINDEG**, choosing among non-unique minimum degree nodes). On the whole, the heuristics do a good job of finding optimal width TDs on **SMALLBINARY**, **SMALLCLIQUE**, and **SMALLCYCLE** (with the exception of **METNND**). The greedy heuristics have trouble finding the optimal width TD on **SMALLPLANAR**, while **LEXM** and **MCS** both find an optimal decomposition on the grid. On **SMALLER**, we observe that the greedy heuristics and **METNND** outperform **LEXM** and **MCS**;

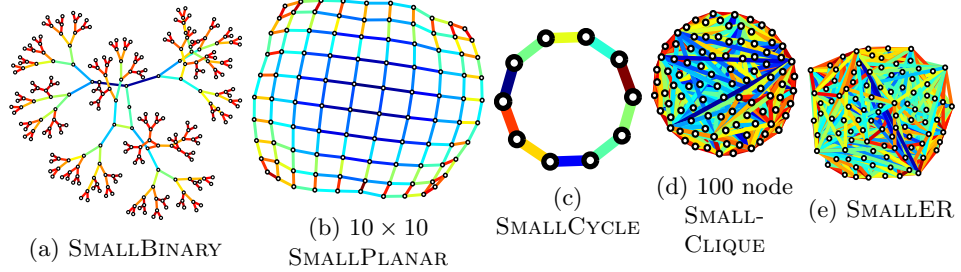


Figure 1: A set of small networks. In this visualization the edges are colored by their length in the planar embedding.

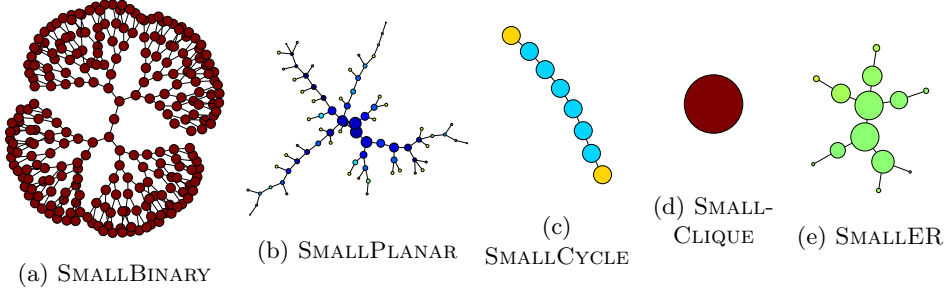


Figure 2: Greedy MINDEG TDs of the toy networks. Bags are colored by the fraction of possible edges present in the bag, with red being denser and blue being less dense.

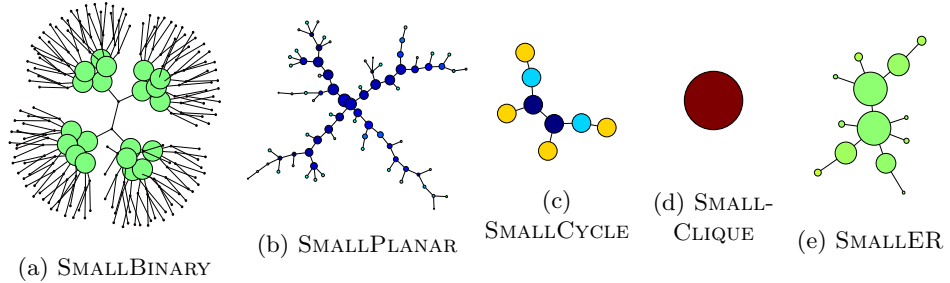


Figure 3: METNND (nested node dissection via METIS) TDs of the toy networks. Bags are colored by the fraction of possible edges present in the bag, with red being denser and blue being less dense.

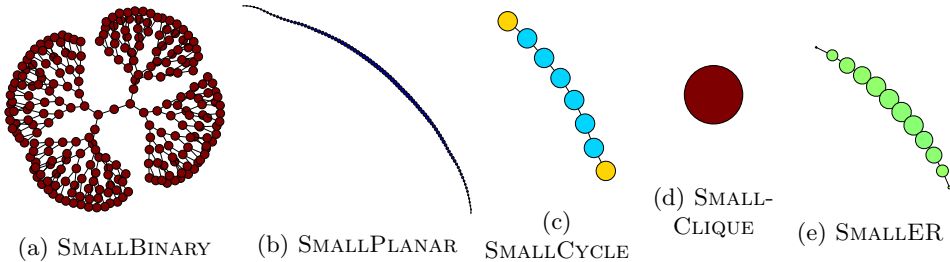


Figure 4: LEXM TDs of toy networks. Bags are colored by the fraction of possible edges present in the bag, with red being denser and blue being less dense.

this is in agreement with previously-reported results [22].

Table 3 shows a summary of our results for the *median* width of TDs produced by various heuristics (as defined near the end of Section 2.2). The median width is potentially more useful for revealing structure in realistic network data since, e.g., it can be used to see whether a TD is dominated by larger bags or by smaller bags. If a network is dominated by bags of small size (such as **SMALLBINARY**, **SMALLCYCLE**, **SMALLPLANAR**), depending on the internal structure of the bag, this can indicate several things. For example, the small bags could consist of tight clusters or cliques, indicating that the network has many tightly connected but *small* groups of nodes. Alternatively, if a small bag’s structure is mostly disconnected, this may indicate the bag is related to small cycles (an example is given below).

For **SMALLCYCLE**, and **SMALLPLANAR**, the small bags are of a cyclical nature, while for **SMALLBINARY** the small bags all consist of 2-cliques. **SMALLCLIQUE** and the **SMALLER** have large median widths (though this is trivial in the case of the clique). The 100-clique is both trivial and too large of a clique to be realistic, but **SMALLER** has interesting bags. As it is a relatively dense network, the bags are connected, but the connections are not tight enough to view any of these bags as a single cluster/community. Importantly, as we will see below, most real networks have a small median width, with the smallest bags dominated by cliques, intermediate bags dominated by cycles, and with large, connected, central bags which resemble the bags of **SMALLER**. The results in Table 2 illustrate this, showing the small median widths of **SMALLPLANAR**, **SMALLCYCLE** and **SMALLBINARY** and the large median widths of **SMALLER** and **SMALLCLIQUE**. Table 2 also demonstrates that, while there are differences in the widths of the TDs produced by the heuristics, these differences are reasonably small.

Network	$n$	$W_{\text{MINDEG}}$	$W_{\text{MINFILL}}$	$W_{\text{NND}}$	$W_{\text{MCS}}$	$W_{\text{LEXM}}$
<b>SMALLBINARY</b>	128	1	1	3	1	1
<b>SMALLPLANAR</b>	100	13	13	14	10	10
<b>SMALLCYCLE</b>	10	3	3	3	3	3
<b>SMALLCLIQUE</b>	100	100	100	100	100	100
<b>SMALLER</b>	100	86	85	86	91	89

Table 2: TD heuristic *maximum* widths. The widths of the **SMALLCLIQUE** and **SMALLER** are relatively large (they grow linearly with the network size), the width of **SMALLPLANAR** network is of an intermediate size (they grow with the square root of the network size), and the widths of **SMALLBINARY** and **SMALLCYCLE** are small (they stay constant with the size of the networks). The greedy heuristics find smaller width decompositions on **SMALLER**, while **LEXM** and **MCS** perform better on **SMALLPLANAR**.

Network	$n$	$\tilde{W}_{\text{MINDEG}}$	$\tilde{W}_{\text{MINFILL}}$	$\tilde{W}_{\text{NND}}$	$\tilde{W}_{\text{MCS}}$	$\tilde{W}_{\text{LEXM}}$
<b>SMALLBINARY</b>	128	1	1	1	1	1
<b>SMALLPLANAR</b>	100	5	5	5	10	8
<b>SMALLCYCLE</b>	10	3	3	3	3	3
<b>SMALLCLIQUE</b>	100	100	100	100	100	100
<b>SMALLER</b>	100	52	51	49	85	80

Table 3: TD heuristic *median* widths. Notice that this measurement is much smaller than the corresponding widths in several of the networks, although it remains large with **SMALLER**. This indicates that most of these networks are dominated by bags which are much smaller than the largest bag in the network.

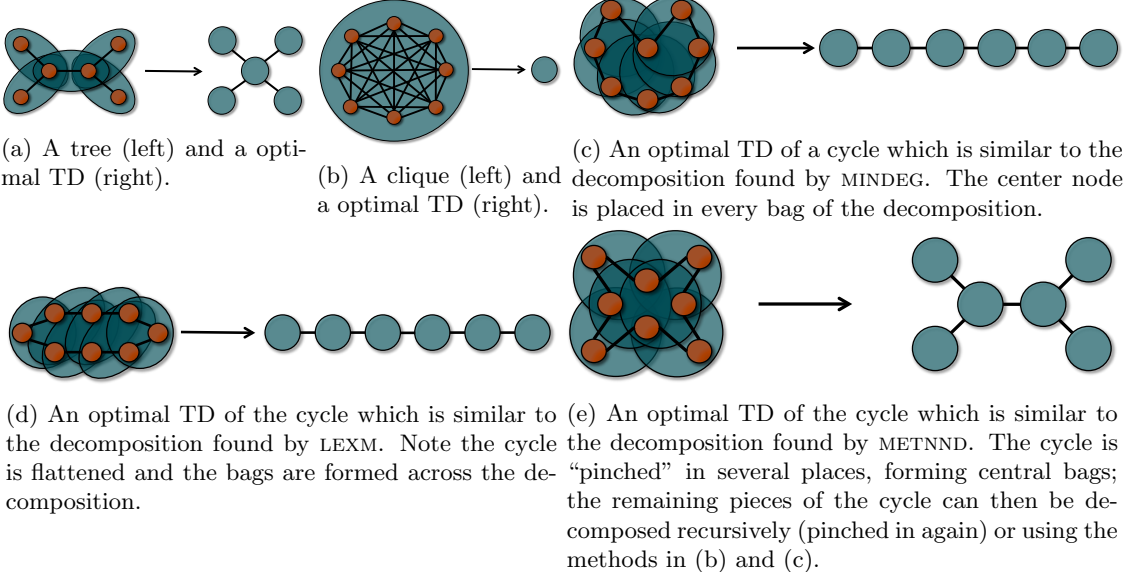


Figure 5: A set of example tree decompositions. The tree and the clique have a standard optimal decomposition. The cycle has many possible minimum width decompositions, though all place disconnected nodes in the bags.

## 4.2 TDs on clique-like and cycle-like toy networks

An important aspect of the behavior of TD heuristics is the difference between their behavior on (denser) clique-like graphs and (sparser) cycle-like graphs. In Figure 5, we illustrate and provide more details on this. First, for reference, in Figures 5a and 5b we give canonical minimum width TDs for a tree and a clique. To understand the difference between cycles and cliques, recall that there are many ways of producing a TD on a cycle (three of these are illustrated in Figures 5c, 5d, and 5e). One simple way is to produce a tree which is a path. This can be done by taking a node  $v$  and placing it and its two neighbors in a bag at one end of the path. Then, keeping  $v$  in every bag, progress around the cycle sequentially forming the next bag by including  $v$  and the two nodes of the next edge (see Figure 5c). Another method produces a path by “flattening” the cycle, and places each edge in a bag with the node from the other side (see Figure 5d). The METNND heuristic “pinches” the cycle at a few points, and the produces branches from each of those points (see Figure 5e).

Although there are many differences between these TD heuristics, a common theme between these different approaches (and one to which we will return below) is that the nodes in the cycle must be placed in bags with nodes they are *not* neighbors of it in the original graph. Relatedly, different heuristics are often very different in terms of how they make this decision, and its effect can be seen in the TDs constructed by these heuristics.

Another important (but related) consideration is the interior structure of each bag that is produced by a TD heuristic. Recall that in SMALLCLIQUE, the only valid TD (which does not contain unnecessary bags) is a single bag containing the entire network. Relatedly, if the network is a  $k$ -tree, formed by overlapping cliques (rather than overlapping edges, as in a normal or 2-tree), then the TD will have bags which consist of the individual cliques. Thus, with cliques, it is the local structure (local in the original graph, in the sense that it is driven by neighbors of a given node in the original graph, in contrast with what is going on in, e.g., SMALLCYCLE) that drives the bag formation. With cycles, on the other hand, this local structure is partially “lost” in the

bags of the TD. This is of interest since, as already mentioned, the interior structure of bags of different widths is important for understanding what is creating the properties of the TD.

As an example, we observe that, for all of the heuristics, the larger bags on **SMALLPLANAR** have many disconnected nodes, and only a few edges. As has been already mentioned, this is a sign of cyclical behavior; and, indeed, from the TD perspective, the grid “looks like” a set of small, regular, overlapping cycles. The structure of the TD is formed by the heuristic’s method of moving across the grid and closing cycles. This suggests that a simple metric to measure whether the interior of a bag is driven by cycles or is driven by small, tightly connected clusters: measure the fraction of edges present in the bag, i.e., the *edge density* of the bag. (We will do this below, and this is why we chose to color many of the visualizations in this section by the density of the bag in question.) Observe, though, that since small bags only have a few possible edges, all else being equal, they will tend to be denser than much larger bags.

### 4.3 TDs on well-partitionable and poorly-partitionable toy networks

**SMALLPLANAR** (for which there exist good well-balanced partitions) and **SMALLER** (for which there do not exist good well-balanced partitions) also illustrate differences between the TD heuristics. For both graphs, the greedy heuristics and **METNND** have significantly smaller median widths than maximum widths. At a high-level, this is indicative of heterogeneity in the network: there are nodes which are so entangled with other nodes that they must appear together in a large bag. But there are also nodes which are connected to only a small number of other nodes and only need to appear in a few very small bags. This can partially be explained by the tendency of the greedy heuristics to work from the “boundary” of the graph (in both of these networks the boundary nodes have small degrees) and to pick points to “eat” into the graph; but it is also true for **METNND** which splits the graph and, to a lesser extent, for **LEXM**.

This is illustrated in Figure 6 for **SMALLPLANAR**. Using **MINDEG** as an example, recall that heuristic works by successively picking a minimum degree node in the network; thus, when applied to **SMALLPLANAR**, it will pick each of the corner vertices of the grid first. This then forms small bags at each corner and, depending on whether it is picking non-unique nodes at random or in an ordered fashion, it will then proceed to work in from the periphery of the network. Indeed, in Figure 2 and 3, we see that the TDs for these heuristics have four major arms with small leaves containing nodes from the border of the grid. Figure 6 provides a visualization of where the nodes from these bags (one of the peripheral bags and one of the central bags in the TD) are in **SMALLPLANAR**. (See, in particular Figures 6a and 6c for the results of **MINDEG**.)

The **LEXM** and **MCS** heuristics, in contrast, find the minimum possible width for the grid, but the TDs—as illustrated in Figure 4 for **LEXM**—that are produced are long, path-like trunks. This is due to the way that **LEXM** picks a starting node and then works across the graph in the style of a breadth-first search. With **SMALLPLANAR**, it starts at one corner and then moves across the network to form a minimal triangulation. Although the (maximum) width is minimal, the median widths of these networks are relatively large, as most of the bags are roughly the same size (see Figures 6b and 6d for the results of **LEXM**).

With **SMALLER** (which is harder to visualize since it doesn’t embed well in two dimensions), the **MINDEG** and **METNND** algorithms also eat in from the “boundary” of the network, where here “boundary” means nodes with *slightly* smaller degrees or *slightly* better cuts (slightly smaller due to random fluctuations). As with the very different **SMALLPLANAR**, this produces several arms and then a few central bags. In **SMALLER**, the greedy heuristics produce a better TD in terms of width than the **LEXM** and **MCS** heuristics, both search based heuristics. While one cannot easily visualize **SMALLER** in a manner similar to Figure 6, these similarities and (substantial) differences between TD heuristics in **SMALLER** (compared with **SMALLPLANAR**) are apparent in

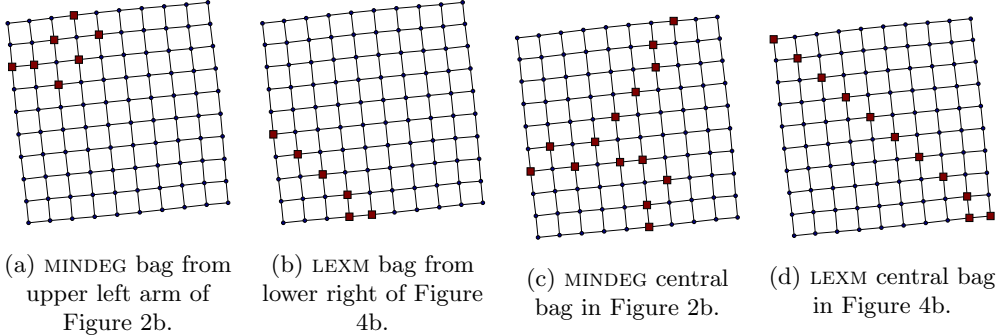


Figure 6: Representative bags from an arm in MINDEG and an arm in LEXM, as well as the associated central bags. In MINDEG, each arm progresses from a different corner of SMALLPLANAR. However, when these bag lines converge, the central bags end-up containing pieces of each line, as in Figure 6c. In LEXM, the line proceeds diagonally across the grid from the lower left corner to the upper right in a regular manner, as in Figure 6d. This results in smaller central bags and produces a path decomposition. See the main text for more details.

Figures 2, 3, and 4.

#### 4.4 Summary of TD results on toy networks

Overall, the greedy heuristics, e.g., MINDEG or METNND, seem to produce a better representation of the large-scale structure of SMALLPLANAR and SMALLER than the LEXM and MCS heuristics in two ways. In SMALLER, the greedy heuristics find decompositions with both smaller maximum as well as smaller median widths. Since most real networks have a randomized aspect to their generation, this indicates that greedy heuristics may be more useful. On SMALLPLANAR, the median width is smaller and the greedy heuristics do a better job of “capturing” all four corners of the grid. In other words, the resulting tree decomposition has four branches, each of which is tied to a specific corner of the network, while LEXM and MCS TDs capture two of the corner structures. Although the maximum width is smaller with LEXM and MCS, the ability to capture what is an obvious visual feature of a simple network is of potential interest.

In the rest of the paper, we will be considering significantly larger and more complicated networks than these toy examples. With these larger networks, the METNND and AMD heuristics, as implemented using INDDGO [27], are the most scalable, compared with the basic greedy algorithms (MINDEG or MINFILL). The AMD heuristic is very related to the MINDEG heuristic (recall that AMD picks minimum nodes based on an easy-to-compute *approximation* of node degree), and it gives similar results to MINDEG. We should note that the implementation of METNND available in INDDGO took longer to complete on some of the real networks. Additionally, the the most consistent difference between the two heuristics seems to be the number of central/overlapping bags produced. Thus, we will often show results only for the AMD heuristic as a matter of visual convenience.

## 5 Tree decompositions of synthetic networks

In this section, we will describe the results of using a variety of TD heuristics on a set of synthetic networks. We focus our attention on two simple classes of random graphs: the popular Erdős-Rényi (ER) random graphs (in Section 5.1); and a power law (PL) extension of the basic ER

model (in Section 5.2). (We emphasize, though, that similar qualitative results also hold for many other random graph models—in their extremely sparse regimes.) This will allow us to begin to understand how TDs behave in random graph models with a very simple random structure. Importantly, we will focus on *extremely* sparse graphs. For the ER model, this means values of the connection probability  $p$  that lead to the graph not even being fully-connected (in which case we will consider the giant component), while for the PL model this means values of the degree heterogeneity parameter  $\gamma$  that are typically used to describe many realistic networks and that lead to analogously sparse graphs.

ER graphs are often presented as “strawmen,” since they obviously do not provide a realistic model for many aspects of real-world networks (e.g., the heavy-tailed degree distributions and the non-zero clustering coefficient present in many real networks). Indeed, “vanilla ER” graphs that are often considered (e.g., ER graphs with densities that are sufficiently large that the graph is fully-connected) are *not* tree-like—either by the metric notion of  $\delta$ -hyperbolicity or by the cut-based notion of TDs. Recent work has shown, however, that with respect to their large-scale structure, *extremely* sparse ER networks do capture several subtle but ubiquitous properties of interest in realistic networks: first, the small-scale versus large-scale isoperimetric structure of the NCP [1, 2]; second, a size-resolved version of  $\delta$ -hyperbolicity that is consistent with large-scale metric tree-like-ness [3]; and third, a non-trivial core-periphery structure with respect to  $k$ -core decompositions [3]. (In particular, in the sparsest regime of the ER networks that we consider, ER(1.6), a very shallow core-periphery structure appears—whereas none exists at the higher densities.) Importantly, for all three of these properties, similar results were seen with other random graph models, such as PL random graphs in the regime of the degree heterogeneity parameter that is commonly-used. Prior work has also provided evidence that these extremely sparse random graphs have nontrivial tree-like structure (at least relative to much denser ER graphs) when viewed with respect to the cut-like notion of tree-likeness [3].

Here, we provide a much more detailed analysis of this phenomenon for TD heuristics applied to ER and PL graphs. We will be particularly interested in similarities between extremely sparse ER graphs and PL graphs with respect to the core-periphery structure (as identified, e.g., from  $k$ -core and related decompositions) of a network. Among other things, we show in this section that this core-periphery structure is captured with the AMD TD. Of particular interest is the how the core-periphery structure relates to central (low eccentricity) or perimeter (high eccentricity) bags in the TD. We will see important similarities between these two classes of graphs, with respect to TD heuristics, and in Section 6 we will use these similarities to help to understand the output of TD heuristics on real-world graphs.

## 5.1 TDs of ER Networks

Here, we give a summary of the empirical results of a more complete analysis of TDs on ER random graphs, with an emphasis on the behavior as the connectivity parameter  $p$  is varied. Recall that, in the very sparse to extremely sparse regime, ER networks have non-trivial global structural changes as  $p$  is varied [97, 98]. In particular, for our subsequent results, there are three regimes of  $p$  that are of interest: if  $p < \frac{1}{n}$ , then the largest connected component is  $O(\log n)$  in size, and the small components are likely trees; if  $\frac{1}{n} < p < \frac{\log n}{n}$ , then the graph has a giant component (i.e., a constant fraction of the size of the network is connected), and the remaining small components of size  $O(\log n)$  are likely trees; and if  $p > \frac{\log n}{n}$ , then almost surely the network is fully-connected, the degrees are very near their expected value, and there are no good-conductance clusters (of any size). We are interested in these last two regimes, and we consider synthetic graphs (ER(1.6) through ER(32)—values of  $p$  between 1.6/5000 and 32/5000, for graphs with  $n = 5000$  nodes) that go from extremely sparse to somewhat denser. Recall that Table 1 provide basic statistics

for these graphs.

### 5.1.1 Visualization and basic statistics

We start with Figure 7 and Table 4, which show the basic features of the TDs of ER networks. Figure 7 presents a visualization of part of the output of a TD with the AMD heuristic, colored by density of bag subgraph, for the sparsest (ER(1.6)) and densest (ER(32)) networks in our ER suite. AMD is selected because of space, and the results are similar to those of METNND. Observe that there is a much greater heterogeneity in the density of bags for ER(1.6) than for ER(32). For the former, there are many small bags which are cliques; while for the latter, there are fewer small bags, and the bags are much sparser in general. This suggests that the sparser ER(1.6) has greater structural heterogeneity than the denser ER(32), which we have confirmed upon inspection.

A more detailed understanding of this can be obtained from the summary statistics in Table 4. Several observations are worth making. First, the number of bags in the TD tends to decrease as the density  $p$  increases (with the exception of the sparsest regime, where the giant component is much smaller). This is because the network is mostly placed into a single bag, with any heuristic, and only a few bags are needed to take care of the remaining nodes. Second, the TD itself, viewed as a graph, has smaller diameter as the density  $p$  increases. Third, the maximum and median width increases with the average degree of the network. Indeed, the width increases quickly with the average degree, with the largest bag (at the “center” of the TD) containing 77% of the nodes in the network in ER(32). Finally, the median density of the bags decreases dramatically as the density of the original graph increases. This perhaps counterintuitive phenomenon is easily-explained by the observation that for extremely sparse ER, the TDs have many small bags which require small numbers of edges to have a reasonably high edge density. With the dense graphs, many nodes have to be placed in each bag, and this requires a quadratically larger number of edges per bag to achieve a similar density.

Network	$N_{\text{AMD}}$	$E_{\text{AMD}}$	$W$	$\tilde{W}$	$\tilde{D}$
ER(1.6)	3127	44	79	1	1.0
ER(1.8)	3457	38	157	1	1.0
ER(2)	3760	38	235	2	0.67
ER(4)	3777	35	1093	3	0.40
ER(8)	2787	29	2208	8	0.20
ER(16)	1856	28	3142	17	0.12
ER(32)	1136	22	3863	33	0.06

Table 4: Basic AMD tree decomposition statistics for ER networks.  $N_{\text{AMD}}$  gives the number of bags in the tree decomposition,  $E_{\text{AMD}}$  gives the maximum eccentricity (diameter) of the tree decomposition,  $W$  and  $\tilde{W}$  are the maximum and median width of the decomposition, and  $\tilde{D}$  is the median bag density.

In light of these results, we would next like to look in more detail at the structure of the TDs generated on these different ER networks (e.g., what changes as we move from the central, large bags of the TD to the smaller, peripheral bags of the TD) as well as the internal structure of each bag. Recall, first, a previous result on the structure of sparse ER networks [88]. It has been shown that in an ER graph with expected degree greater than  $2 \log 2$ , but still sufficiently sparse, there are three different parts of the random network (two parts which may be viewed as core-like, one part which may be viewed as periphery-like) [88]. The core-like part of these graphs is bi-connected, and it has an expander-like inner core (i.e., a set of nodes of “higher”

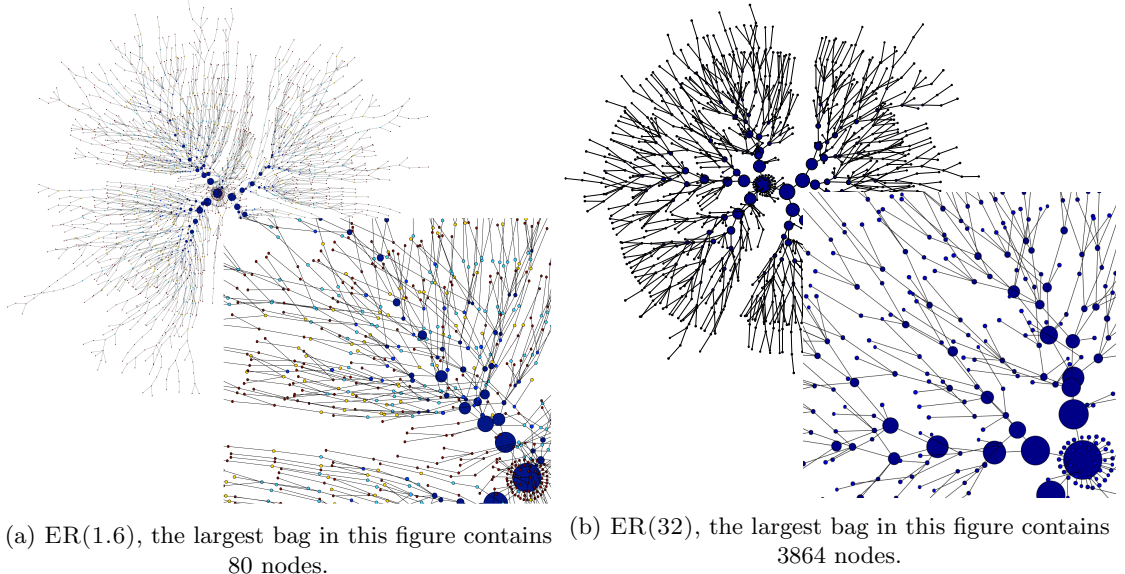


Figure 7: Visualization of ER(1.6) and ER(32) AMD tree decompositions, colored by the density of the bag subgraph. For visualization purposes, the two networks are not drawn to the same scale. The bags in ER(32) have widths that are approximately 50 times larger than that of ER(1.6). The blowups show the upper-left corner of the visualization in greater details. The blowups show the color of some of the smaller bags that are in the peripheral part of each TD. In ER(1.6), many of the very small bags are red (meaning they contain a clique, the vast majority of which are simply a single edge). Slightly larger bags are light blue or yellow (indicating an edge density of ca. 0.25 (light blue) to ca. 0.75 (yellow)). In ER(32), all of the bags of the TD are dark blue, indicating that these bags are all very sparse, regardless of whether they are peripheral or central to the TD. Table 4 confirms this.

degree), surrounded by an outer core which has long chains of nodes (forming sparse cycles). The third, peripheral, part of the network consists of tree “whiskers” that hang off the biconnected core. A similar structure has been observed empirically when looking at low-conductance clusters/communities in a wide range of large social and information networks [1] and also when looking at the Gromov hyperbolicity and  $k$ -core properties of these real-world networks [3]. This contrasts sharply with the denser ER graphs which are much more regular in terms of their degree variability, core structure, etc. Our results (here on extremely sparse ER graphs and below on PL graphs and many real-world graphs) demonstrate that TD heuristics can reflect this core-periphery structure.

### 5.1.2 Internal bag structure

Next, consider Figure 8, where we present visualizations of three typical AMD bags for ER(1.6) and ER(32), respectively. In each case, the three bags are the most central (lowest eccentricity) bag in the TD (which we call the central bag), a typical bag that is a leaf in the TD (which we call a periphery bag), and a typical bag that is in between these two in the TD (which we call an intermediate bag). In these two figures, the color-coding is by  $k$ -core number, with high core nodes being red and low core nodes being blue. The most prominent thing to note about these figures is that the central bag for ER(1.6) is disconnected and consists of almost all singletons, while the central bag for ER(32) is well-connected; and that the intermediate and peripheral

bags for ER(1.6) are small, the latter consisting of only a single edge, while for ER(32) both the intermediate and the peripheral bag has non-trivial internal structure.

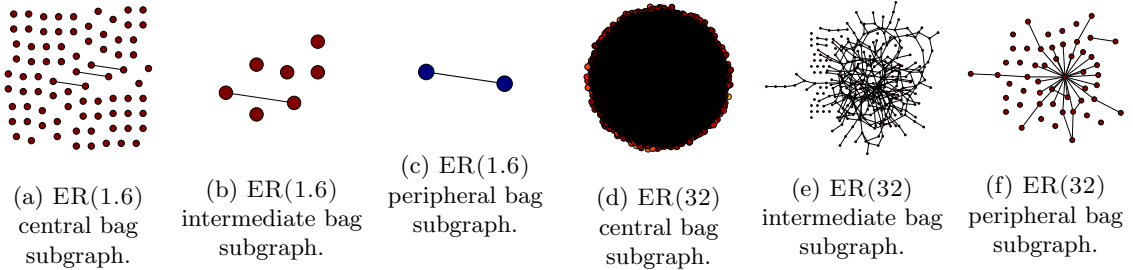


Figure 8: Bag subgraphs of a AMD TD of ER(1.6) and ER(32) graphs, colored by the  $k$ -core number of the node (red is high  $k$ , blue is low  $k$ ). The central bag is the largest bag in the TD and one of the bags of minimum eccentricity; the peripheral bag is a leaf in the TD graph, and it achieves the minimum width in the TD; the intermediate bag is in between these two extremes.

The increased density of ER(32) over ER(1.6) is the obvious cause of these differences, but it is worth considering what structures, produced by the increased density, affect the formation of the AMD TD. For example, recall from the toy graphs that heuristic TDs of cycles produced bags which had disconnected nodes. There were several different ways of producing the decomposition, but any TD of a small width on a cycle includes disconnected nodes in most bags. The more complex PLANAR, has many small overlapping cycles. In its case, the heuristics have to put many nonadjacent nodes into a bag. One way of thinking of this is that cycles force distant nodes into the same bag and that many overlapping cycles will force many distant nodes into the same bag.

This intuition suggests (and we have confirmed by inspection) that a bag with many disconnected nodes, as in the central bag of ER(1.6) shown in Figure 8a, is due to a large number of overlapping cyclical structures. The intermediate bags of ER(1.6) contain nodes from the long, overlapping cycles of the outer core (and as these cycles do not overlap as much in periphery, these bags have fewer nodes), while the peripheral bags each contain a single edge, capturing the small trees on the periphery of the network (see also Figure 7). The coloring of the nodes indicates the core-periphery structure of the subgraph induced by the bags. In ER(1.6) there is only a 1-core (blue) and a 2-core (red), thus the red nodes in the central bags are all in the 2-core, while the peripheral trees are in the 1-core, which agrees with [88].

On the other hand, in ER(32), whose core-periphery structure spans from a 7-core (blue) to a 23-core (red) though almost all of the nodes (94%) are in the 23-core, the central bag contains a relatively tightly-connected mass of 77% of the nodes in the network. This begins to look more like SMALLER, which is a very dense ER network. The intermediate bags contain sparser structures (with some of the disconnected nodes and edges that are indicative of cyclical structures); and, although the peripheral bags still contain the smallest structures, in ER(32) they no longer contain only a single edge. This indicates that even the sparsest regions contain cycles and other complicated structures, but very few triangles, which agrees with the small clustering coefficient of these networks.

### 5.1.3 Large-scale organization

In order to provide a more quantitative evaluation of these ideas (which will enable comparison in the next section with the real-world data), and to characterize better the large-scale organization

of these synthetic networks, consider Figures 9, 10, and 11. These three figures plot bag cardinality histograms, average bag density versus bag cardinality (recall that this is the width + 1), and average  $k$ -core versus bag eccentricity for two ER networks (as well as a suite of PL and real-world networks—we will refer to other subfigures below, but for now consider only Figures 9a and 9e, Figures 10a and 10e, and Figures 11a and 11e for results on ER(1.6) and ER(32), respectively.)

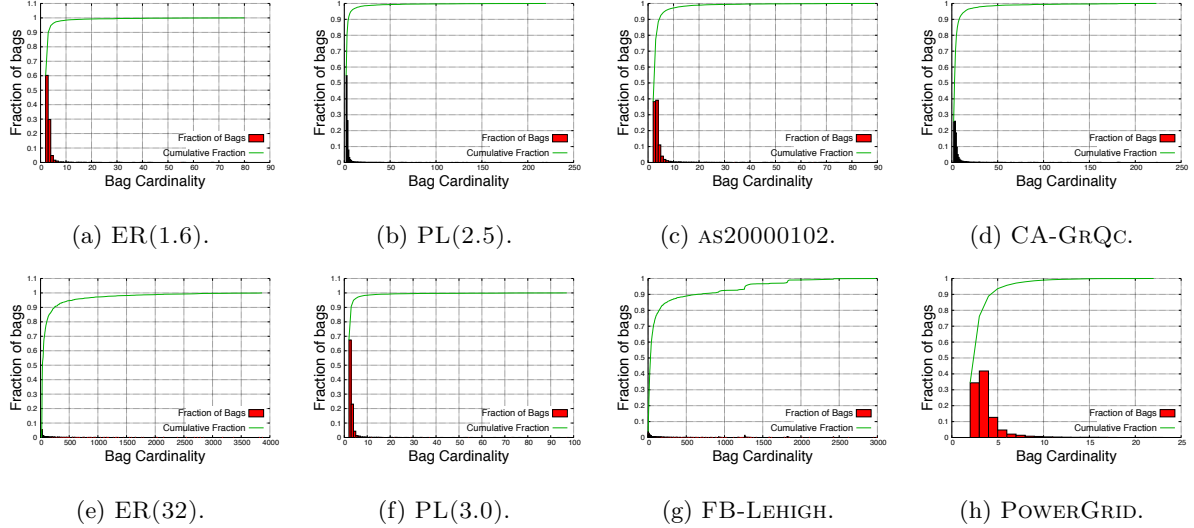


Figure 9: Bag cardinality histograms with cumulative fraction of bags for a representative set of networks. For all of the networks, there are many more small cardinality bags than large cardinality bags. This is consistent with a TD structure which has a few central bags which quickly taper and branch off into many small peripheral bags. As we will see in Figures 10 and 11, in networks with a strong core-periphery structure (e.g., not POWERGRID), these peripheral bags tend to have a low average  $k$ -core and high relative density. FB-LEHIGH has the most large bags, due to the tendency of the FB networks to form long, path-like trunks in its TDs. POWERGRID has the smallest tapering effect; although the largest bags are still at the center of the decomposition, there is only a small change in size from the largest bags to the smallest, presumably since this network has the weakest core-periphery structure.

We saw in Figure 8a the central bag for ER(1.6), and we interpreted it in terms of the output of AMD TD as due to overlapping cycles; the histograms in Figure 9a show that for ER(1.6) (and the networks in the rest of Figures 9) there are only a very few such central bags. On the other hand, Figure 9 also shows that there are many very small bags in ER(1.6). Two features we noticed about these two types of bags are that there is a change in edge density between the large and small bags and that there is a change in the  $k$ -cores represented between the large and small bags. The associated ways of measuring this are shown in Figure 10 and Figure 11, where the average edge density of a bag is plotted against the bag cardinality. These figures show that small peripheral bags are dense (relative to their small size—in the extreme case, this could be a single edge), and they contain low  $k$ -core nodes, as indicated, e.g., by the downward slope of the plots in Figure 11a.

Many of the results for ER(32) are very different than for ER(1.6). For example, the histograms in Figure 9a show that this network has a much larger proportion of high-width bags than ER(1.6). The largely homogeneous nature of the core-periphery structure of dense ER networks should also be clear since the nodes, no matter what size bag we choose, are mostly

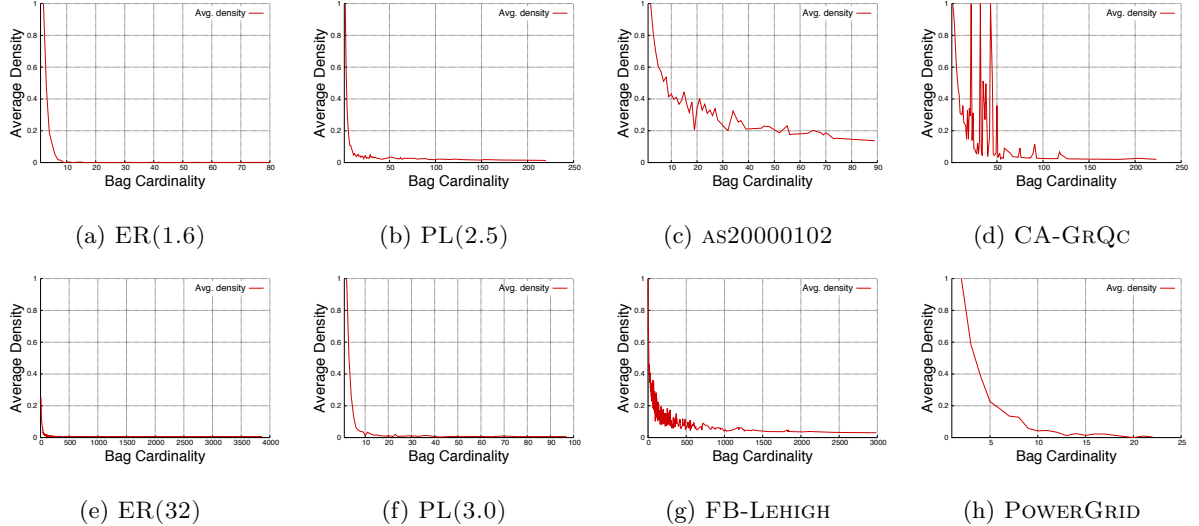


Figure 10: Average bag density versus bag cardinality plots for a representative set of networks. In the PL networks the small bags are dense—in the extreme case consisting of a single edge—like the ER(1.6) network; but the largest bags are larger and mostly connected, similar to the intermediate and central bags of ER(32). The real-world networks all show denser bags even at large size scales as compared to the synthetic networks, and this is due to the increased clustering present in these networks.

in the deepest core ( $k = 23$ ). These trends can be seen by comparing the density of the smallest bags in ER(1.6) and ER(32) in Figures 10a and 10e. The flat plot of the average  $k$ -core in Figure 11e, which holds steady close to the value of the maximum  $k$ -core, indicates the lack of a core-periphery structure in the network.

Putting all of these results together, we can conclude that when it exists (e.g., in extremely sparse ER graphs), the core-periphery structure of ER networks is captured by the AMD TD; and when the core-periphery structure does not exist (e.g., for ER graphs for other even moderately sparse values of  $p$ ), the large width of the TD indicates that the most of the network is in the largest bag, which is analogous to the fact that most of the nodes are in the core of the network.

## 5.2 TDs of PL Networks

Here, we give a summary of results of an analysis of TDs on PL random graphs, with an emphasis on the behavior as the degree heterogeneity parameter  $\gamma$  is varied and how properties of the TDs correlate with core-periphery structure. Recall that Table 1 provide basic statistics for the PL graphs we consider. PL graphs are a class of random graphs that are ER-like, except that degree heterogeneity is exogenously-specified; and previous work has shown that PL graphs have important similarities with extremely sparse ER graphs when one is interested in small-scale versus large-scale tree-like structure [1, 3, 2]. In particular, the increased degree heterogeneity produces a large-scale core-periphery structure in the PL networks, similar to the extremely sparse ER networks, but these PL networks also have some of the characteristics of denser ER networks (e.g., the core is more strongly connected and the diameter of the network is smaller). As we will see, TDs show the ability to capture this structure in a similar manner to the ER networks.

We start with Table 5, which show the basic features of the TDs of PL networks. PL(3.0) has the least amount of degree heterogeneity and has similar characteristics to ER(1.6), while

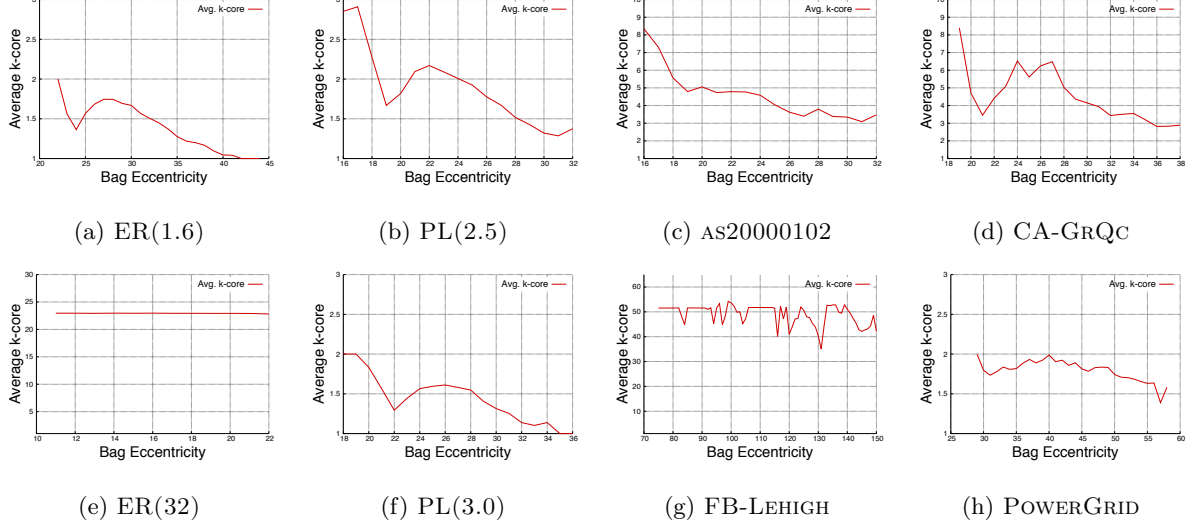


Figure 11: Average  $k$ -core versus bag eccentricity for a representative set of networks. The correlation between the core-periphery structure and the central-perimeter bags can be seen in a downward slope in these plots. Networks with no prominent core-periphery structure (ER(32) and POWERGRID, for two very different reasons) have a flat plot here; while networks with moderate core-periphery structure (the PL graphs and ER(1.6)) have a downward sloping line, but relatively shallow (i.e., not deep) cores. AS20000102 and CA-GRQC both have prominent, deep core-periphery structures that reveal themselves in this plot. The dips that show up at small eccentricities in several of the synthetic networks and CA-GRQC are due to the many small ‘‘whiskers’’ (in the sense of [1]) that hang off of the core bag. FB-LEHIGH also has a deep core-periphery structure (in the sense of  $k$ -core decompositions); but because of the long path-like nature of the TD and since most of the nodes are in the deepest cores, the plot is flat with larger downward dips as the bag eccentricity increases.

the lower degree exponents (PL(2.75), PL(2.5)) have characteristics similar to both the dense and sparse ER networks. Most notably, the maximum width increases (as it would if the density increased), while the median width and median bag density stay the same (low and high, respectively), as in the ER(1.6). In the previous section, we saw that the low median width and high density was related to the presence of a core-periphery structure in the network. As we will see, this is also true of the PL networks, and the AMD TDs are again able to capture this structure.

Interestingly, among other things, we find that for the PL networks, for a given average degree, the presence of very high degree nodes that tend to link to each other means that the density of the high-width bags, i.e., the core of the network, is greater, making it more like the cores of the denser ER networks. On the other hand, the peripheries of these PL networks are still very sparse, and TD bags including them look more like the peripheries of the sparse ER networks. The periphery results are reflected in the results presented in Table 5, where we see that the median width is low and the median density is high (many bags with only a single edge within). The visualizations of the central, intermediate, and peripheral bags from TDs of PL networks in Figure 12 also reflect this. In particular, the central bag for PL(2.5) looks somewhat like the intermediate ER(32) bags, while the central bag for PL(3.0) is much less well-connected; and the peripheral bags for both PL graphs look like the ER(1.6) bags. Again, the tree decomposition reflects the core-periphery structure via the central-peripheral bags as reflected in the downward

Network	$N_{\text{AMD}}$	$E_{\text{AMD}}$	$W$	$\tilde{W}$	$\tilde{D}$
PL(2.5)	4672	32	219	1	1.0
PL(2.75)	4500	39	148	1	1.0
PL(3.0)	3974	36	96	1	1.0

Table 5: Basic AMD tree decomposition statistics for PL networks.  $N_{\text{AMD}}$  gives the number of bags in the tree decomposition,  $E_{\text{AMD}}$  gives the maximum eccentricity (diameter) of the tree decomposition,  $W$  and  $\tilde{W}$  are the maximum and median width of the decomposition, and  $\tilde{D}$  is the median bag density.

slope of Figure 11b.

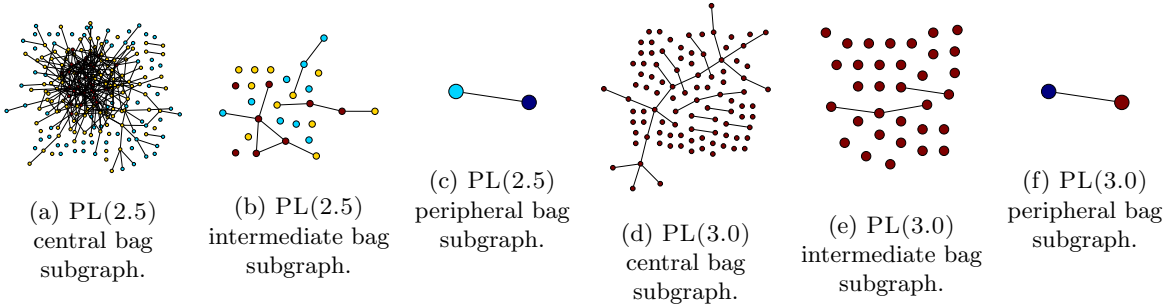


Figure 12: PL(2.5) AND PL(3.0) bag subgraphs, colored by  $k$ -core number of the node.

As the power law exponent  $\gamma$  is increased, recall that the amount of degree heterogeneity in the resulting network is reduced, i.e., the number of high degree nodes specified by the power law degree distribution is decreased. As a necessary consequence of maintaining this distribution as the nodes are connected, the high degree nodes are likely to be connected to other high degree nodes. This causes a core-periphery structure to emerge (see [3] for empirical measurements between the relationship between  $\gamma$  and the  $k$ -core structure).

For example, the core-periphery structure of PL(3.0) is shallower than that of PL(2.5), as seen in Figure 11. Similarly, the width of the PL(2.5) AMD TD is larger than that of the PL(3.0) AMD TD. Interestingly, in all cases these widths are less than the corresponding ER(2) network, whereas one might expect these networks to have larger widths because of the increased core-periphery structure. This occurs because there are several factors to consider as  $\gamma$  is decreased. The core *does* become denser as more edges are added to the core, causing these nodes to become more difficult to separate, but most of those extra edges come from the outer regions of the expander-like core, thus shrinking the size of the core and increasing the size of the periphery. In other words, when only a few medium degree nodes are added, then there are still cyclical structures in the core, as is observed in ER(1.6), except smaller; but as higher degree nodes are added, the core becomes denser and begins to become larger, as this forces larger and larger pieces of the core to be placed in the same bag, as is observed in ER(32).

The TD results on ER and PL graphs demonstrate that TDs (in particular, with the AMD heuristic) can capture the core-periphery structure of two common random network models. In both cases, to the extent that there was a core-periphery structure (which itself depended on the sparsity parameter  $p$  or the degree heterogeneity parameter  $\gamma$ ), the central and peripheral bags in the TD from AMD were correlated with this structure. The peripheral bags were smaller and much sparser than the central bags and contained nodes from the shallow (low)  $k$ -cores of

the network. With the exception of the tree-like periphery of the extremely sparse ER and the PL networks, the structures observed in TDs of the random network models were largely driven by loosely connected core structures (e.g., overlapping loops in sparser regions and expander-like cores in the denser regions). This is consistent both with the results on the toy networks and previous work involving the structure of ER networks [97, 88]. (The one exception to this is the denser ER(32), where the central bag contained 77% of the network; in this case, the network does not exhibit the core-periphery structure of the other networks looked at in this section.) We will see how we obtain similar results when applying the AMD heuristic to real world networks.

## 6 Tree decompositions of real-world networks

In this section, we will describe the results of using a variety of TD heuristics on a set of real-world networks. Our goal is to use the insights from the previous sections to evaluate the performance of existing TD heuristics on real social and information networks and to understand how those TDs can be used to obtain an improved understanding of the properties of these realistic networks. Our main results are three-fold.

- First, in Section 6.1, we summarize the results of a detailed empirical evaluation of the AMD TD heuristic applied to our suite of realistic networks. The main focus will be on illustrating how these TDs can capture previously-identified large-scale core-periphery structure, and also illustrating how the internal structure of the TD bags can be understood in terms of properties like large-scale cycles and small-scale clustering in the original graph.
- Second, in Section 6.2, we evaluate the ability of the AMD TD heuristic to identify small-scale good-conductance communities such as those previously-identified by the NCP with local spectral methods [1, 2]. In particular, we will show connections between bags that are more peripheral in the TD and small good-conductance communities responsible for “dips” in the NCP.
- Third, in Section 6.3, we illustrate that TD heuristics can be used to identify certain other types of large-scale non-conductance-based “ground truth” communities. In particular, we will show connections between bags that are more central in the TD and large-scale community-like (by a “ground truth” metric but not by conductance quality) clusters.

### 6.1 Results on identifying core-periphery structure

Here, we will describe the results of an empirical evaluation of the AMD TD heuristic applied to our suite of realistic networks (the real-world networks in Table 1). We will begin in Table 6 with a brief survey of all of our real networks, and we will then focus on four representative networks: AS20000102, CA-GRQC, FB-LEHIGH, and POWERGRID. The first three of these representative networks all exhibit some form of previously-recognized core-periphery structure [3], while POWERGRID is known to lack a strong core-periphery structure (basically because the network is heavily tied to the underlying locally-Euclidean geometry of the Earth [3]). Note, though, that the Facebook networks are very core-heavy, in the sense that they have many nodes in deep cores, essentially because of their significantly higher average degree (see, e.g., [3] and Table 1). (Thus, informed by previous results on  $k$ -core decompositions and related tree-like techniques [3, 74, 1, 86], we expect to see evidence of the core-periphery structure in the TDs associated with AS20000102, CA-GRQC, and, to a lesser extent, FB-LEHIGH, but a lack of substantial core-periphery structure in the TD of POWERGRID.)

### 6.1.1 Overview of core-periphery results for all networks

Let us start with our summary statistics in Table 6. In this table, we present the number of bags in the AMD TD ( $N_{\text{AMD}}$ ), the maximum eccentricity (diameter) of the TD ( $E_{\text{AMD}}$ ), the maximum and median width of the TD ( $W$  and  $\tilde{W}$ , respectively), and median bag density ( $\tilde{D}$ ). These measurements provide us with an idea of how large is the most connected part of the network (maximum width); how numerous are small bags (median width), which is indicative of areas of the network that have small separators, in our case small peripheral regions of the network; and whether the small separators are more clique-like or consist of mostly disjoint nodes (median density), with disjoint nodes being indicative of cycles and clique-like structures being indicative of more meaningful communities. We note that a large maximum width combined with a low median width is evidence for a deep core and a shallow periphery, and that high median density is evidence for a periphery based on more community-like separators, rather than more disparate separators. We note that these observations assume that high density bags are mostly small-width bags. This assumption is plausible, given that as the width  $w$  of a bag increases, the number of edges required to maintain a constant density increases like  $w^2$ ; and in many cases we have confirmed this assumption indirectly or by direct observation. For example, see our discussion of bag density and bag width below, as well as Figure 10 below for empirical evidence that high density bags are generally the smallest width bags.

Network	$N_{\text{AMD}}$	$E_{\text{AMD}}$	$W$	$\tilde{W}$	$\tilde{D}$
CA-GRQC	3014	39	222	2	1.0
CA-ASTROPH	10708	78	3616	5	1.0
AS20000102	6364	33	88	2	1.0
GNUTELLA	6475	33	1629	2	0.67
EMAIL-ENRON	26781	78	2237	3	1.0
FB-CALTECH	395	30	357	18	0.53
FB-HAVERFORD	516	56	891	37.5	0.38
FB-LEHIGH	1919	151	2983	31	0.32
FB-RICE	1481	76	2553	31	0.37
FB-STANFORD	4809	100	6674	16	0.38
POWERGRID	4666	59	21	2	0.67
POLBLOGS	899	49	294	6	0.57
ROAD-TX	$1.25 \times 10^6$	170	197	3	0.5
WEB-STANFORD	$2.10 \times 10^5$	500	1419	5	0.83

Table 6: Statistics for TDs of real networks.  $N_{\text{AMD}}$  gives the number of bags in the AMD TD;  $E_{\text{AMD}}$  gives the maximum eccentricity (diameter) of the TD;  $W$  and  $\tilde{W}$  are the maximum and median width of the TD; and  $\tilde{D}$  is the median bag density.

Networks based on an underlying Euclidean geometry (e.g., ROAD-TX, POWERGRID) have low maximum widths and low median widths, which indicates that they do *not* have a strong core-periphery structure. While these networks have many small width bags, which is indicative of tree-like sections of the network, the internal subgraphs have a low median density (e.g., as compared to certain ER networks), indicating the presence of many disparate paths into the interior. More social networks, such as POLBLOGS and the Facebook networks, all have higher average degrees and, consequently, higher widths, with lower median widths. Again, this is one indicator of a core-periphery structure. As the median widths are higher in these networks, as compared to the other real networks (although the median widths are lower than the associated ER networks), the peripheral structure in these social graphs tends to be denser than in the other networks. Also, the median density, while low compared to the other real networks, is very high

compared to the median density of the densest ER networks in Table 4. Thus, although the periphery is more difficult to separate into small good-conductance community-like clusters than some of the other real networks, e.g., CA-GRQC or CA-ASTROPH, it is still formed from more community-like pieces than similar ER (or PL) networks.

Observe also that the two web networks, GNUTELLA and WEB-STANFORD, have high widths, like the Facebook networks, but lower median widths; and that they have higher median densities (especially when compared to ER(4), ER(8), and ER(16)). This indicates that these networks have a sparser, more tree-like periphery than other social networks, which is also consistent with previous results [1]. Importantly, and also consistent with previous results [1], is that the sparsest, most tree-like peripheries belong to the collaboration, email, and autonomous systems networks (CA-GRQC, CA-ASTROPH, EMAIL-ENRON, AS20000102). These networks all have low median widths, high median densities, and high maximum widths, indicating that they exhibit the cleanest core-periphery structure; this is also consistent with the previously-observed upward-sloping NCPs of these networks [1, 2].

### 6.1.2 More details on core-periphery structure of four representative networks

To supplement the summary statistics that we presented in Table 6 for all of our networks, we will now look at several representative networks in greater detail. Let us start by discussing Figures 9, 10, and 11, from Section 5. Figure 9 clearly shows that most of the bags in the TDs are small-width bags and that there are only a few large bags. In fact, proportionally, FB-LEHIGH has the largest fraction of large bags, and yet 80% of the bags are below width 200 (in a graph with 5073 nodes, where the TD has a maximum width bag of 2983). Since the bags and edges of TDs form separators in the network, this indicates that there are many relatively small separators. These are the largest in Facebook networks, where the separators tend to have around 100 nodes, while in most other networks many of the separators have around 10 nodes. This is consistent with typical views of core-periphery structure, with a few more highly-connected nodes in the core and many less well-connected nodes in the periphery. That is, in order to separate off most pieces of the periphery (where “piece” is defined by the end of branches in the TD), only 10 or fewer nodes are needed for most of the social/information networks, while ca. 100 nodes are needed for the Facebook networks.

In Figure 10, we see the average edge density for bags of a given cardinality plotted against the bag cardinality (which, recall, equals width + 1). The results of this figure confirm that the small-width bags have high densities. An important distinguishing feature of the three representative real networks (that are not tied to an underlying Euclidean geometry) is that the curve has a heavier tail than in the synthetic networks. This indicates that separators, up to much larger size scales, are less disparate (e.g., are denser or clumpier) than in the synthetic networks. In POWERGRID, on the other hand, the underlying Euclidean geometry leads the density to fall off more quickly. Interestingly, it falls off similarly to the sparse ER network, except that the tail of the curve is shorter. Thus, in this case, only the smallest bags have tight separators.

In Figure 11, we consider the relationship between the core structure and low eccentricity (central) bags, and we compare that with the relationship between the periphery structure and the high eccentricity (perimeter) bags in the TD. In particular, Figures 11c and 11d show that for AS20000102 and CA-GRQC there is a clear downward trend as the bag eccentricity is increased. This indicates that low eccentricity bags contain more high  $k$ -core nodes on average and that the high eccentricity bags contain more low  $k$ -core nodes on average. Figure 11g shows that FB-LEHIGH, due to its greater density, has a mostly flat profile until the most extreme reaches of eccentricity are met, at which point some of the bags begin to contain nodes of a lower  $k$ -core. Thus, the core-periphery structure is present in FB-LEHIGH, but the core-periphery structure is

moderated by a very large core which produces long path-like sets of nodes that in turn leads to large core bags and hence a much larger eccentricity for this TD. (We note that this is typical of the results for most of the Facebook networks, which is consistent with their flat NCP [2].) Finally, POWERGRID, which is not expected to have exhibit a correlation between  $k$ -core structure and bag eccentricity, has a flat profile.

To illustrate some of these findings pictorially, we present visualizations in Figures 13 and 14. These figures consider a central or very deep core bag, a perimeter or very peripheral bag, and an intermediate bag, for each of our four representative networks; and these figures show the community-like nature of typical bags for the three representative information networks, i.e., AS20000102, CA-GRQC, and FB-LEHIGH, as well as the more disparate separators of the POWERGRID. The coloring of the visualizations in these figures is by  $k$ -core: the red nodes are in deep (high)  $k$ -cores while the blue nodes are in shallow (low)  $k$ -cores.

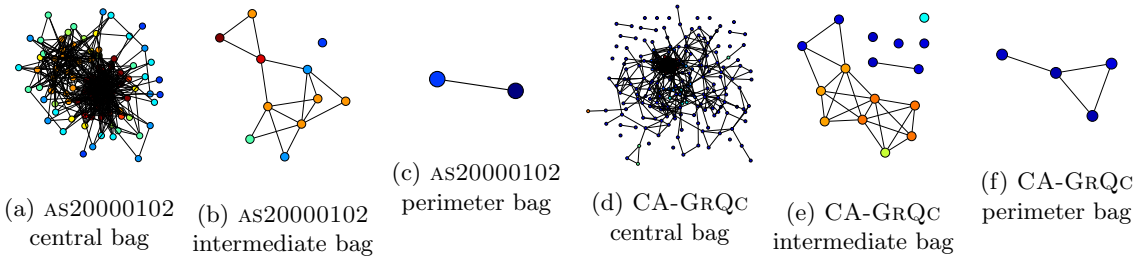


Figure 13: AS20000102 and CA-GRQC AMD bag subgraphs, colored by  $k$ -core number, with red indicating deep/high  $k$ -cores and blue indicating shallow/low  $k$ -cores.

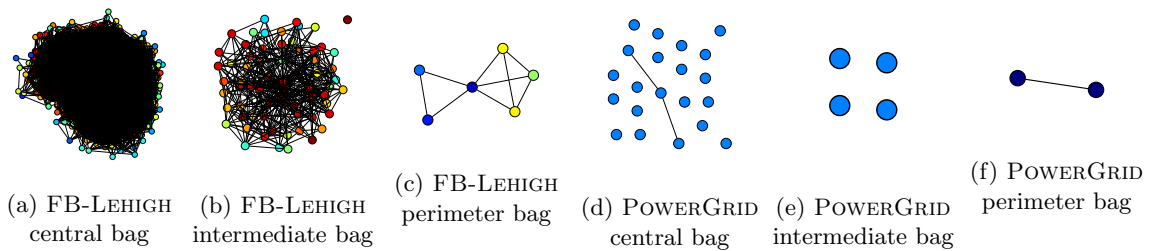


Figure 14: FB-LEHIGH and POWERGRID AMD bag subgraphs, colored by  $k$ -core number, with red indicating deep/high  $k$ -cores and blue indicating shallow/low  $k$ -cores.

One final observation we would like to make is to address the “dips” in the average  $k$ -core curves shown in Figure 11 (e.g., the dip in Figure 11d at a bag eccentricity of 21 or in Figure 11g throughout). These dips are due to what we will call “twigs,” where a twig is a small (low width and short) branch off of a much larger (high width and long) trunk-like structure of the TD. For example, in FB-LEHIGH and in the other Facebook networks, the high average degree results not only in high widths, but in larger collections of bags of high width. These are arranged in a long path (a “trunk”) with many branches at either end. Along this main trunk, there are occasional twigs which contain peripheral nodes. Since the trunk is long, the average  $k$ -core at the point where the twig is attached is slightly lower, resulting in the dip in the curve. In Figure 15, we provide a visualization of the twigs responsible for three of these dips.

### 6.1.3 Summary of large-scale core-periphery and tree-like structure in real-world networks

Taken together, these empirical observations suggest that many realistic social/information networks have a nontrivial core-periphery structure; and that in many cases this is caused by many small overlapping cluster-like or moderately clique-like structures. That is, there is local non-tree-like structure that “fits together” into a global core-periphery structure that is tree-like (in a metric and/or cut sense) when viewed from large size scales. This is in sharp contrast with many models and intuitions. Most obviously, this is in contrast with the random networks (in particular, the not extremely sparse ER networks and to a lesser extent the PL networks, but many other more popular random generative models) which have a locally tree-like, but globally loopy structure. (Among other things, this more expander-like random structure manifests itself in the TDs in the sparse bag subgraphs and the lack of a core-periphery structure.) Less obviously, this is also in sharp contrast with networks such as POWERGRID, PLANARGRID, and ROAD-TX that are strongly tied to an underlying Euclidean geometry. Said another way, many realistic social/information networks have a more tightly-connected core-like structure than is present in typical random networks, and they have peripheral and intermediate regions that are “clumpier” than these random networks. While these claims are perhaps intuitive, our empirical observations demonstrate that they can be meaningfully identified with TDs and interpreted as leading to large-scale cut-based tree-like structure.

Interestingly, aside from the local clumpiness, the real-world social/information networks do have a core-periphery structure that is reminiscent of that which is also seen in extremely sparse ER graphs and PL graphs with greater degree heterogeneity. (This too is consistent with prior results suggesting that extreme sparsity coupled with randomness/noise is responsible for the dips in the NCP [1, 2].) It is also worth emphasizing that in most of the intermediate bags of the real social/information networks, there are still a small number of disconnected nodes. This indicates that there are still a small number of alternate paths, which are disparate from the clusters, to the rest of the nodes in the network. The most prominent exceptions to these general observations are networks that either do not have a strong core-periphery structure, e.g., POWERGRID that is tied to a two-dimensional underlying Euclidean geometry, or networks that have a relatively low clustering coefficient, e.g., GNUTELLA09. In both of these cases (but for different reasons), the internal subgraphs of the intermediate and peripheral bags have a larger number of disconnected nodes than the other realistic networks.

## 6.2 Connections with good-conductance communities results

Here, we will consider how the peripheral part of the tree-like core-periphery structure identified by TDs relates to low-conductance clusters/communities that were previously-identified by the NCP method [1, 2]. To do so, observe that one way to determine whether a TD “captures” clustering/community structure is to see if those clusters/communities are well-localized in the TD. By “well-localized,” we mean here that the cluster/community is contained in a relatively small number of (contiguous) bags. Since the NCP method (which plots the best communities at different size scales [1, 2]) finds good low-conductance communities with a local spectral personalized page rank (PPR) method [99], we followed previous local spectral procedures to generate a set of candidate clusters [1, 2]. Then, given a set of candidate clusters, we looked at how many bags in the TD contain at least one node from this cluster, i.e., we measured how well-localized the community is in the TD. As a crude threshold of whether a cluster/community is localized, we

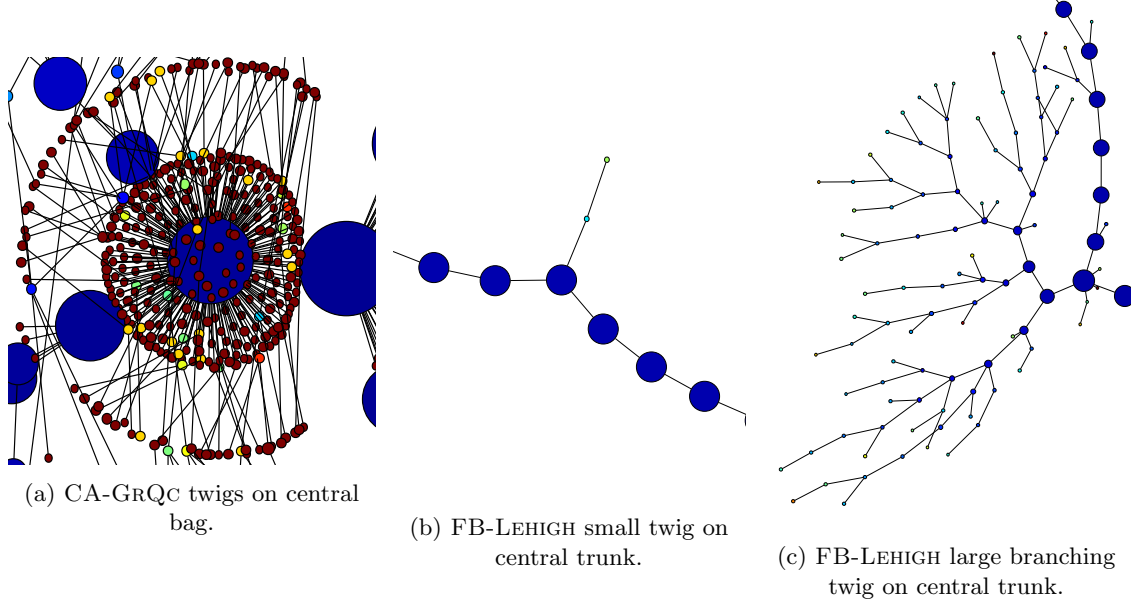


Figure 15: Twigs on the the FB-LEHIGH and CA-GRQC networks. The bags are colored by the density, with blue indicating low density and red indicating high density. A small twig and a larger, branching twig on the FB-LEHIGH trunk are shown. These twigs, combined with the extremely long, path-like trunk, cause the dips in the  $k$ -core eccentricity plot. In CA-GRQC, the concentration of the twigs on one or two central bags causes only a single, large dip as compared to the multiple dips in FB-LEHIGH. The synthetic networks in Figure 11, (PL(2.5), PL(3.0), and ER(1.6)) also have twigs similar to CA-GRQC.

consider it to be localized if it is contained in fewer bags than there are nodes in the community.<sup>9</sup> We apply this method using the AMD heuristic.

Our results for several real-world and synthetic networks are presented in Figures 16–20. For each figure and subfigure, the horizontal axis represents a community size in number of nodes (on log scale), and the vertical axis is either the conductance of the best community found using the PPR method (recall that conductance is a ratio of edges leaving the community to the total number of edges which have an endpoint in the community [1, 2], and thus a low conductance represents a better community) or the number of number of bags that contain members of the community (again, on log scale). In addition, in the bag plots, the red line represents the number of bags which contain a node *from the community in corresponding NCP plot*, and the green dashed line represents the locality threshold. Thus, when the number of bags for a given community is localized by our definition, the red plot will be below the green threshold.

As a reference point, consider the extremely sparse and somewhat denser ER networks, which are shown in Figure 16. Since it is so sparse, ER(1.6) does have some very small good-conductance clusters. As shown in the figure, however, the small “communities” are contained in roughly the same number of bags as there are in the community. This is expected, as these communities are

<sup>9</sup>To understand why this threshold was chosen, consider the following example: if a community of size  $n$  is a tree, e.g., whiskers in ER(1.6), then it will be contained in  $n$  bags in the (ideal) TD; if the community is a “clique whisker,” i.e., a clique connected to the rest of the network by only one edge, it will be contained in just one or two bags; and if the community contains deep core nodes which are connected to many nodes outside of the community, the community will be spread across many bags in the network. We examined other measures of TD locality, which showed similar results.

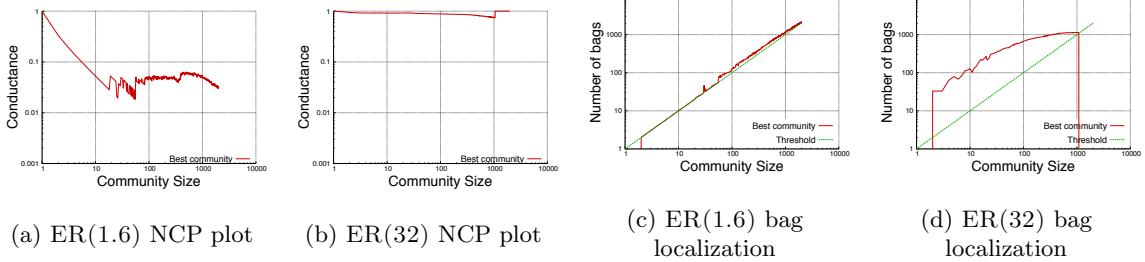


Figure 16: ER(1.6) and ER(32) NCP plots and tree localization plots. The localization threshold is plotted in green.

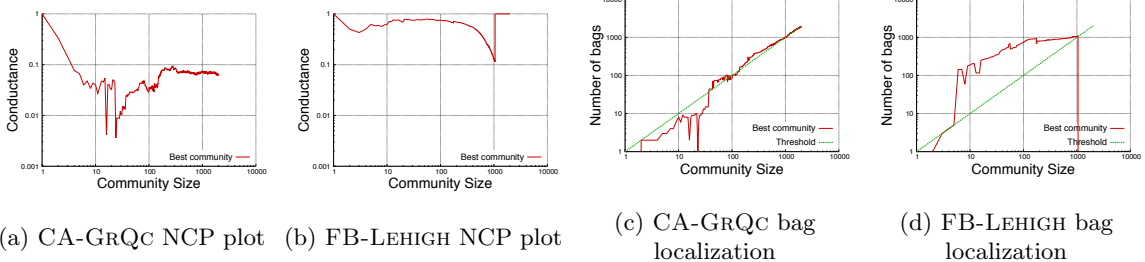


Figure 17: CA-GRQC and FB-LEHIGH NCP plots and tree localization plots. The localization threshold is plotted in green.

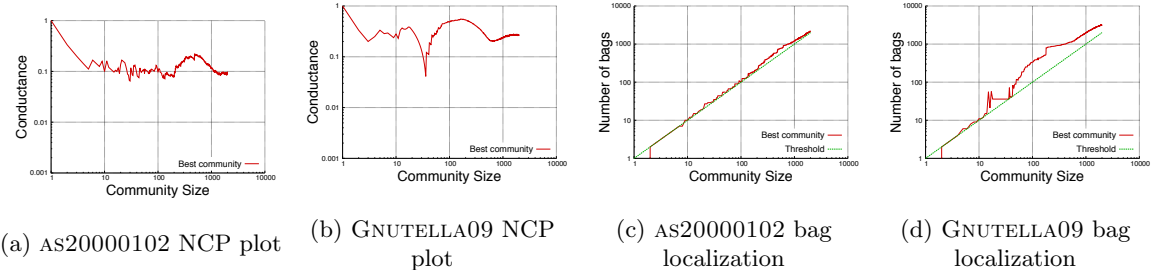


Figure 18: AS20000102 and GNUTELLA09 NCP plots and tree localization plots. The localization threshold is plotted in green.

largely peripheral tree-like whiskers in the network (see Section 5). For the larger communities, which include core nodes, the localization is slightly above the line defining our threshold. On the other hand, for the denser ER(32), there are no good-conductance clusters at any size, and the bag localization is far to very far above the line defining the localization threshold, indicating that the localization is poor to very poor at all size scales.

For the small and intermediate-sized clusters in many of the real networks, and in particular many of those from the large-scale empirical analysis of [1], the smaller good-conductance clusters found using the PPR method are reasonably well-localized within the TD, while the larger poorer-conductance clusters are not. Consider, e.g., CA-GRQC in Figure 17 as an example of this. On the other hand, both large and small clusters found with the PPR method applied to the denser

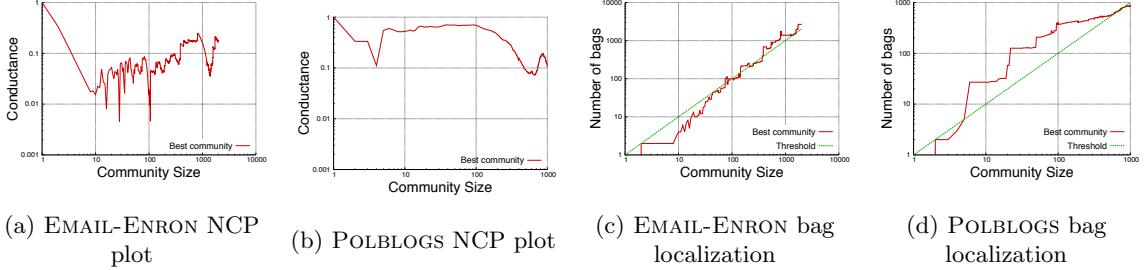


Figure 19: EMAIL-ENRON and POLBLOGS NCP plots and tree localization plots. The localization threshold is plotted in green.

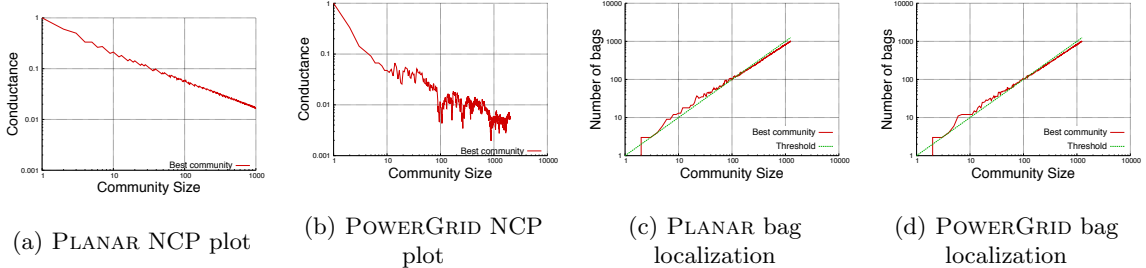


Figure 20: PLANAR and POWERGRID NCP plots and tree localization plots. The localization threshold is plotted in green.

graphs from the FACEBOOK100 set (i.e., those that do not have even small-cardinality good-conductance clusters [2]) are not well-localized in the TD. Consider, e.g., FB-LEHIGH in Figure 17 as an example of this. Figure 18 shows AS20000102 and GNUTELLA09, which also shows NCP plots that do not yield small good conductance clusters, and which shows that the outputs of the PPR method are not particularly well-localized in the TD. Figure 19 shows that EMAIL-ENRON does have some of its small good-conductance clusters well-localized in the TD, and it also shows that the output of the PPR algorithm applied to POLBLOGS leads to medium-to-large clusters with poor conductance values that are poorly-localized in the TD.

Finally, although networks with an underlying Euclidean geometry are of less interest for social/information network applications, for completeness it is worth considering how these TD methods apply to them. Figure 20 presents results for PLANAR and POWERGRID. Both of these networks have downward-sloping NCP plots which are different from the other social and information networks, reflecting the Euclidean geometry underlying these networks. In both cases, fairly uninteresting results are obtained, suggesting that the localization metric we propose is more interesting for realistic social graphs with nontrivial tree-like core-periphery structure.

Although our results demonstrate that good-conductance clusters/communities in several realistic social graphs are well-localized in TDs found with existing heuristics, it is not obvious how to address the reverse question of finding good-conductance communities from a TD. One could attempt to look at all or some large number of combinations of bags in the TD. Since one is usually interested in well-connected communities/clusters, the running intersection property of TDs could be used to restrict attention to connected subsets of a TD. There are, however, two obvious issues. First, there does not exist an obvious analogue of the “sweep cut” used in the spectral partitioning method for finding the best community from a TD. Second, as a related

practical matter, the presence of high degree (or deep core) nodes in the intermediate and central bags of a TD cause bags to be poor conductance communities. These nodes have many connections and increase the “surface area” of most cuts, even if there is only a small number of them in a cluster. We observed that, in the clusters we found using the PPR method, each cluster is typically well-represented by a set of small bags plus a couple of nodes in the larger bags. If we then attempt to form clusters by combining bags, we get *all* of the nodes in the larger bags, including deep core nodes. Additional methods of filtering nodes for the larger bags, such as ordering by node degree or  $k$ -core combined with a sweep cut may improve these results.

### 6.3 Results on identifying ground-truth communities

Here, we will consider other ways in which the output of TDs can be useful in identifying clusters/communities of interest to the domain analyst. First note that the results of the previous subsection might seem to suggest that larger bags constructed from existing TD heuristics do not capture meaningful structures or communities in realistic networks. We have, however, in many cases observed otherwise; and here we describe two examples from the demographic data associated with the Facebook100 dataset [91].

Consider, first, Figure 21, where we show the AMD TD of the FB-HAVERFORD network, and where each bag is colored-coded by the average graduation year of the constituent nodes. The first thing to observe is that there is a large linear or trunk-like structure that dominates the large-scale structure of the TD. Not surprisingly, we observe that there is a strong overlap between the nodes that comprise successive bags in that trunk. Moreover, we note that this trunk-like structure is typical of most of the FACEBOOK100 networks (but is not seen in most other social graphs we have considered). The second thing to observe is that each end of the long trunk correlates strongly with graduation year and that there is a gradual change in the average graduation year of each bag as we move across the trunk. Thus, to the extent that one accepts graduation year as some sort of easily-quantifiable “ground truth” community, the large bags in the TD of this network seem to be capturing a legitimate ground-truth structure in the network. This fits well with prior results that report that in most of the Facebook networks graduation year is best predictor of the existence of edges between two nodes [91].

Consider, next, Figure 22. It is known that for a small number of the FACEBOOK100 networks (e.g., FB-CALTECH, FB-RICE, and FB-UCSC), residence hall rather than class year is the best edge predictor [91]. To see how this manifests itself in TDs, we considered the AMD TD of FB-CALTECH. (Actually, we considered the students-only subset of FB-CALTECH, since non-students, e.g., alumni and staff, are less likely to depend on a college residence hall for social structure.) In this case, a single simple trunk-like structure is not dominant, but there are several relatively large peripheral branches, and many of the peripheral branches are dominated by a particular residence hall. In Figure 22, the bags are colored by the fraction of students who listed residence hall 170 (chosen arbitrarily) as their residence. These examples are of particular interest since good-conductance clusters do not exist in FACEBOOK100 networks [2].

By looking at bags where the concentration of a particular community node is higher than the incidence of that community throughout the TD, we can form a very simple classification rule by looking at contiguous subtrees formed from these bags. In more detail, given residence hall  $X$ , we collected all bags whose fraction of nodes which were listed as belonging to residence  $X$  was higher than the fraction of nodes belonging to that hall in the network (the incidence in the network is given in column  $F$  in Tables 7 and 8). We then kept the largest contiguous set of bags and used membership in this set as the classifier. Although this is an overly simple classifier, the goal in this section is simply to provide a baseline about how the residence communities are located in the TD.

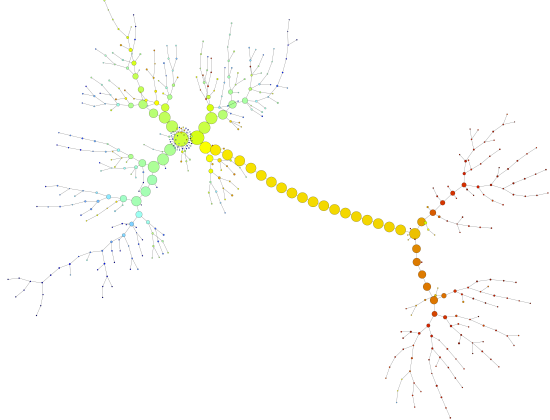


Figure 21: AMD TD of FB-HAVERFORD, colored by graduation year (red = freshman, blue = alumni). The long, path-like trunk of this (and other) Facebook networks is driven by the propensity of students to be friends with students of a similar graduation year. FB-HAVERFORD is presented in this section, rather than FB-LEHIGH (which has similar large-scale TD structure), because its smaller eccentricity (56 rather than 150) makes it easier to visualize.

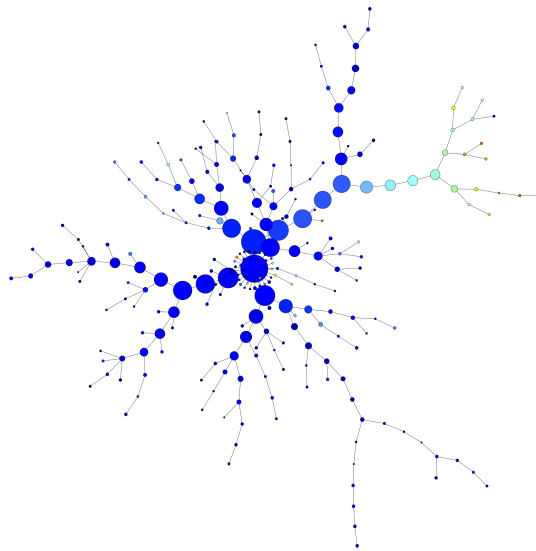


Figure 22: AMD TD of (the students-only subset of) FB-CALTECH, colored by the fraction of students in residence hall 170 (blue = no nodes belong to residence, ..., red = all nodes belong to residence). This is a graphical representation of data presented in Table 8 for the AMD TD and residence hall 170.

We performed this procedure on the students-only restriction of FB-CALTECH. Tables 7 and 8 provide a summary of the classification results using this method on FB-CALTECH network, with the (anonymized) listed residence hall for that student as the community. In more detail, Table 7 shows the fraction of the “ground truth” community captured by the largest contiguous set of bags described above. This is analogous to the recall of classifying the community using this branch in the TD. Table 8 shows the fraction of the nodes in the union of all bags in this largest contiguous set which belong to the community. This is analogous to the precision of classifying

the community using this branch. Since FB-CALTECH is a very small network, we can use a much larger variety of TD as classifiers than is possible for larger networks, and we present results for all of these TD classifiers.

Hall	<i>F</i>	MINDEG	MINFILL	LEXM	MCS	AMD	METNNND
None	.134	.270	.257	.270	.324	.284	.297
165	.066	.472	.528	.556	.528	.472	<b>.861</b>
166	.090	.736	.736	<b>.925</b>	.811	.642	.792
167	.134	<b>.642</b>	.566	.453	.585	.491	.566
168	.116	.746	.762	<b>.952</b>	.889	.825	.143
169	.136	.726	.712	<b>.904</b>	.877	.658	.740
170	.090	.725	.725	.739	.783	<b>.855</b>	.362
171	.136	.714	.673	.776	<b>.857</b>	.592	.429
172	.098	.630	.630	.534	.699	.548	<b>.863</b>

Table 7: Fraction of each FB-CALTECH residence hall captured in the largest contiguous set of “frequent” bags. A frequent bag is a bag where the fraction of students who belong to the given residence hall is greater than the fraction of students who belong to that residence in the entire network. Column *F* gives the fraction of students who identified as being in the associated hall in the entire network (i.e., the threshold for being a frequent bag for that residence hall). This procedure was also performed for the nodes which did not have a residence hall listed for comparison.

Hall	<i>F</i>	MINDEG	MINFILL	LEXM	MCS	AMD	METNNND
None	.134	.065	.064	.068	.071	.071	.100
165	.066	.055	.057	.052	.052	.059	<b>.086</b>
166	.090	.104	.110	.111	.111	.092	<b>.129</b>
167	.134	<b>.102</b>	.097	.092	.087	.088	.092
168	.116	.137	.140	.150	.147	<b>.157</b>	.043
169	.136	.150	.151	.147	.163	.138	<b>.187</b>
170	.090	.134	.139	.145	.140	<b>.171</b>	.103
171	.136	<b>.105</b>	.099	.100	.104	.084	.074
172	.098	.131	.129	.100	.137	.115	<b>.199</b>

Table 8: Fraction of the nodes contained in the largest contiguous set of frequent bags for a given residence hall which *actually belong* to the given residence hall. A frequent bag is a bag where the fraction of students who belong to the given residence hall is greater than the fraction of students who belong to that residence in the entire network. Column *F* gives the fraction of students who identified as being in the associated hall in the entire network (i.e., the threshold for being a frequent bag for that residence hall). This procedure was also performed for the nodes which did not have a residence hall listed for comparison.

Although the communities do seem to be well-captured by the TDs, we should note that there are also many other nodes in the same bags as these communities (see Table 8). Interestingly, although the only bags selected were bags where the residence hall in question was over-represented, combining these bags actually resulted in a lower concentration of residents than were present in the network for some residence halls (see Table 8 where the values are lower the *F* for a given residence hall). This occurs since the non-resident nodes in each of these bags are different, while the resident nodes are largely the same for each bag in the branch.

In terms of heuristic performance, the MINDEG, MINFILL, and AMD seem to have similar performance given a residence, although there seems to be a larger gap between AMD than the

other heuristics. This is not surprising as these are all greedy heuristics which work by reducing fill (or minimum degree, which is a proxy for fill) in each step. LEXM and MCS also seem to behave similarly (again, these two heuristics are based on a breadth-first search of the graph) and they have the best performance in terms of recall (Table 7). METNND has a different profile from the other networks and seems to do the best in terms of precision (Table 8). These results are comparable to what can be obtained with other simple classification rules, and they suggest that TDs could be useful in these types of machine learning applications.

Overall, these results demonstrate that, at least in these types of realistic social/information networks, several types of plausible “ground truth” communities are well-correlated with the large-scale structure identified by existing TD heuristics. This striking since these heuristics make local greedy decisions about how to form the TDs, and it suggests that improved results could be obtained in this application by considering TD heuristics designed for graphs with this type of structure.

## 7 More details on tree decomposition methods

In this section, we consider the question of whether TDs and their treewidths can be related to other parameters for tree-like structure, specifically the Gromov  $\delta$  hyperbolicity.<sup>10</sup> It might appear that there is no relation between TDs and  $\delta$  (since, e.g., treewidth and  $\delta$  take on opposite extremal values on cliques and cycles), but there are in fact structural characterizations for when they align. We will present here our new theoretical results on relating TDs and  $\delta$ -hyperbolicity. Although this result is a relatively-straightforward extension of previous work [100], and although most of the rest of the paper can be understood without this result, we include it here for completeness for the following two reasons: first, since motivating prior work in [3] demonstrates an empirical connection between the cut-based tree-like notion from TDs and the metric-based tree-like notion from  $\delta$ -hyperbolicity; and second, since our results in Section 6 demonstrate the inadequacy of a naïve optimization of treewidth and the importance of large cycles for realistic social graphs.

### 7.1 Treewidth, Treelength, and Hyperbolicity

We start with the following definition, which provides another quality measure of a TD; this was first introduced by Dourisboure and Gavoille [67].

**Definition 4.** Let  $\mathcal{T} = (\{X_i\}, T = (I, F))$  be a tree decomposition of a graph  $G$ . The length of  $\mathcal{T}$  is defined to be  $\max_{i \in I, x, y \in X_i} d_G(x, y)$ , where  $d_G(x, y)$  is the shortest path distance in  $G$ . Analogously to treewidth, the treelength of  $G$ , denoted  $tl(G)$ , is the minimum length achieved by any tree decomposition of  $G$ .

It is straight-forward to see that the treelength is at most the diameter of  $G$ . Like with treewidth, finding a tree decomposition achieving minimum length (and in fact the treelength itself) is NP-hard [68]. Given this, one might ask whether treelength and treewidth can be simultaneously approximated. For general graphs, Dourisboure and Gavoille proved a negative result.

**Theorem 2.** [67] Any algorithm computing a tree decomposition approximating the treewidth (or the treelength) of an  $n$ -vertex graph by a factor  $\alpha$  or less does not give an  $\alpha$ -approximation of the treelength (resp. the treewidth) unless  $\alpha = \Omega(n^{1/5})$ .

---

<sup>10</sup>As we mentioned in Section 2, there has been recent theoretical and empirical interest in this and related questions; see, e.g., [65, 66, 67, 68, 69, 70, 71, 72, 73].

The specific examples used by [67] to prove their negative result are modifications of the 2-dimensional mesh (i.e., a lattice), which—due to long induced cycles—is not  $\delta$ -hyperbolic for small values of  $\delta$ . This suggests that the situation might be very different for “real-world” graphs—which have small diameter and which have non-trivial embedding properties into low-dimensional hyperbolic spaces. (This is an open area of research more generally.) Furthermore, Chepoi et al. [101] showed that if  $tl(G) \leq \lambda$ , then  $G$  is  $\lambda$ -hyperbolic, and conversely, a  $\delta$ -hyperbolic graph  $G$  on  $n$  vertices satisfies  $tl(G) \leq 17 + 12\delta + 8\delta \log_2 n$ . Unfortunately, for many real networks of interest, this is *not* an improvement on the trivial bound of diameter as their diameter alone will be less than  $O(\log_2 n)$ . We conjecture that under minimal additional conditions, a  $\delta$ -hyperbolic graph with diameter  $D$  has treelength at most a function of  $\log_2 D$ , a vast improvement on both known bounds.

In light of this discussion, we turn to the question of using additional structural properties to characterize the interplay between  $\delta$ ,  $tw(G)$ , and  $tl(G)$ . The following theorem is our main result; this theorem follows from the work of Müller on atomic tree decompositions [100], and the proof of this theorem may be found in Section 7.2.

**Theorem 3** (Reidl, Sullivan). *Say a subgraph  $H$  of  $G$  is geodesic if  $d_H(u, v) = d_G(u, v)$  for all  $u, v \in V(H)$ . Let  $\nu(G)$  be the length of a longest geodesic cycle in  $G$ . Then*

$$\delta(G) \leq tl(G) \leq (tw(G) + 1) \cdot \nu(G).$$

Further, this result is tight—there is a graph class  $\mathcal{G}$  of unbounded treewidth and containing arbitrarily long geodesic cycles such that  $\delta(G) = \Theta(tw(G) \cdot \nu(G))$  for every graph  $G \in \mathcal{G}$ .

In other words, if we can eliminate long distance-preserving cycles and obstructions to low treewidth (large grid minors), then our network will embed well in low-dimensional hyperbolic space.

## 7.2 Proof of Theorem 3

Before we can give the proof of Theorem 3, we need a few additional definitions. First, given a rooted tree  $T$  and a node  $s \in T$ , define  $T_s$  to be the subtree of  $T$  with root  $s$ :

$$T_s := T[\{t \in T \mid s \text{ is an ancestor of } t\}].$$

For a graph  $G = (V, E)$  with tree decomposition  $(\{X_i\}, T)$  where  $T$  is rooted arbitrarily, for  $s \in T$  define  $G_s := G[\bigcup_{t \in T_s} X_t]$  to be the graph induced by those bags that are below  $X_s$  in the decomposition. We will write  $N(S)$  for the neighbors of a set  $S$ —more precisely,  $N(S) = \{u \in V \mid (u, s) \in E \text{ for some } s \in S\} \setminus S$ . Finally, for notational convenience, for  $x \in V$  and  $e \in E$ , we will write  $G - x$  for the graph  $(V \setminus \{x\}, E)$  and  $G - e$  for the graph  $(V, E \setminus \{e\})$ . We now define a special type of tree decomposition (so-called *atomic tree decompositions*), and give a crucial property of all vertices that co-occur in one of its bags.

**Definition 5.** [*atomic tree decomposition*, as in [102]] Let  $G$  be a graph on  $n$  vertices. The fatness of a tree decomposition of  $G$  is the  $n$ -tuple  $(a_0, \dots, a_n)$ , where  $a_h$  denotes the number of bags that have exactly  $n - h$  vertices. A tree decomposition of lexicographically minimal fatness is called an *atomic tree decomposition*.

**Proposition 1.** [Lemma 3.9 in Müller [100]] Let  $(\{X_i\}, T)$  be an atomic tree decomposition of a connected graph  $G = (V, E)$ . Then for any two distinct vertices  $x, y$  that occur together in some bag  $X_t$ , either  $(x, y) \in E$  or there exists a neighbor  $s$  of  $t$  in  $T$  such that  $\{x, y\} \subseteq V_s \cap V_t$ .

We also need the following proposition, which follows easily from Lemmas 3.7 and 3.8 in Müller [100].

**Proposition 2.** *Let  $(\{X_i\}, T)$  be an atomic tree decomposition of a connected graph  $G$ ,  $e = (s, t) \in E(T)$  be any edge and let  $T_t$  be the connected component of  $T - e$  rooted at  $t$ , and set  $X = X_s \cap X_t$ . Then there exists a connected component  $C_t$  in  $G_t \setminus X$  such that  $N(C_t) = X$  and  $X_t \subseteq C_t \cup X$ .*

Finally, we are ready to give a bound on treelength in terms of a graph's treewidth and its longest geodesic cycle. Our proof relies heavily on tools from [100].

**Theorem 4** (Reidl, Sullivan). *For any graph  $G = (V, E)$  it holds that  $tl(G) \leq \nu(G) \cdot (tw(G) + 1)$  where  $\nu(G)$  is the length of the longest geodesic cycle in  $G$ .*

*Proof.* We will prove a stronger statement, namely that *any* atomic tree decomposition of a two-connected graph has treelength at most  $\nu(G) \cdot (tw(G) + 1)$ . Let us first show how this proves the lemma for graphs that are not two-connected.

Assume  $G$  is not two-connected and  $x \in V$  is a cut vertex ( $G - x$  has at least two connected components). Let  $H_1, \dots, H_\ell$  be the connected components of  $G - x$ . If we prove that the graphs  $G[H_i \cup \{x\}]$ ,  $1 \leq i \leq \ell$  have tree decompositions  $\mathcal{T}_i$  with treelength bounded as in the statement of the lemma, then we can easily construct a tree decomposition for  $G$  with the same property: we simply introduce a single new bag  $V_x = \{x\}$  and connect it to an arbitrary bag containing  $x$  in each of the individual tree decompositions  $\mathcal{T}_i$  (since these graphs all contain the vertex  $x$  such a bag must exist). Note that the treelength of this decomposition is simply  $\max_{1 \leq i \leq \ell} tl(\mathcal{T}_i)$  since the bag  $V_x$  we added contains only the vertex  $x$  and thus cannot increase the treelength. Since we will show the statement for two-connected graphs in the following, we recursively decompose the graph  $G$  over cut vertices until the remaining connected components are all two-connected and then construct a tree decomposition of  $G$  as described above.

We may now assume  $G$  is two-connected. Given an atomic tree decomposition  $(\{X_i\}, T)$  of  $G$ , we show that for every two vertices  $x, y$  that occur in a common bag  $X := X_t$ ,  $x$  and  $y$  are connected by a path whose length depends only on  $|X|$  and  $\nu(G)$ . To this end, let  $\mathcal{C}_X$  be the collection of geodesic cycles in  $G$  that have at least one vertex in  $X$ . We first show that if  $G[\mathcal{C}_X]$  is connected and  $X \subseteq V(\mathcal{C}_X)$ , then every pair of vertices in  $X$  is connected by a path of length at most  $|X| \cdot \nu(G[\mathcal{C}_X])$ .

Consider  $x, y \in X$ . Start a breadth-first search (bfs) from  $x$  that stops as soon as it reaches  $y$ . Let  $L_1, L_2, \dots, L_p$  be the layers of the bfs-tree where  $L_1 = \{x\}$  is the starting layer. We claim that for all  $L_i$  with  $L_i \cap X \neq \emptyset$ , there is a  $j$  such that  $i < j \leq i + \nu(G[\mathcal{C}_X])$  and  $L_j \cap X \neq \emptyset$ . Consider such an  $L_i$ , and denote by  $X_l \subseteq X$  those vertices of  $X$  that are contained in  $\bigcup_{k=1}^i L_k$ . Denote by  $X_r = X \setminus X_l$  those vertices of  $X$  that have not been visited until step  $i$ . If there exists a geodesic cycle  $C$  in  $\mathcal{C}_X$  with vertices in both  $X_l$  and  $X_r$  we are done – the bfs will have seen all of  $C$  in at most  $\nu(G[\mathcal{C}_X])$  steps (and thus found  $C \cap X_r$ ). Otherwise, since  $\mathcal{C}_X$  is connected, there exist two geodesic cycles  $C_l, C_r \in \mathcal{C}_X$  with  $C_l \cap X_l \neq \emptyset$ ,  $C_r \cap X_r \neq \emptyset$  and  $C_r \cap C_l \neq \emptyset$ . Since the bfs will visit all vertices of  $C_r \cup C_l$  in at most  $(|C_r| + |C_l|)/2 \leq \nu(G[\mathcal{C}_X])$  steps, the claim follows. Therefore the number of layers  $p \leq \nu(G[\mathcal{C}_X]) \cdot |X_t|$  and thus the distance between  $x$  and  $y$  is bounded by  $\nu(G[\mathcal{C}_X]) \cdot |X_t|$  as claimed.

Therefore, if we show that for every bag  $X$ , the set  $\mathcal{C}_X$  of geodesic cycles touching  $X$  induces a connected graph  $G[V(\mathcal{C}_X)]$ , we are done: then every vertex pair  $x, y \in X$  is indeed connected by a path of length at most  $\nu(G[V(\mathcal{C}_X)])|X|$ , which (by the definition of treewidth and the fact  $\mathcal{C}_X$  is a family of geodesic cycles) is bounded by  $\nu(G)(tw(G) + 1)$ .

We first prove that for any choice of  $X := X_t$  and any pair of vertices  $x, y \in X$ ,  $x$  and  $y$  lie on some cycle of  $G$ . By Proposition 1, the vertices  $x, y$  are either connected by an edge (in which

case we are done:  $G$  is two-connected, so every edge lies on some cycle) or there exists some node  $s \in N_T(t)$  such that  $\{x, y\} \subseteq V_s \cap V_t$ . In the latter case, we invoke Proposition 2: for  $i \in \{s, t\}$  we can find connected components  $H_i$  of  $G_i \setminus X$  such that  $N(H_i) = X$  and  $V_i \subseteq H_i \cup X$ . Therefore, there exist two  $x$ - $y$ -paths: one inside  $H_s$  and another in  $H_t$ , hence  $x$  and  $y$  lie on a cycle.

Since the set of geodesic cycles forms a basis for the cycle space of a graph, it follows that for every  $t \in T$ ,  $G[V(\mathcal{C}_{X_t})]$  is connected. The distance between any vertices in  $X_t$  is thus bounded by  $\nu(\mathcal{C}_{X_t}) \cdot |X_t|$ , implying that  $tl(G)$  is at most  $\nu(G) \cdot (tw(G) + 1)$ , as claimed.  $\square$

Finally, we put all the pieces together and show why these bounds are tight.

**Proof of Theorem 3** This follows directly from Theorem 4, Chepoi's result that hyperbolicity is at most the treelength, and the observation that for any non-negative integers  $n$  and  $k$ , the  $k$ -subdivision of the  $n \times n$  planar grid has treelength  $n(k + 1)$ , treewidth  $n$ , a longest geodesic cycle of length  $4(k + 1)$ , and hyperbolicity  $(n - 1)(k + 1) - 1$ .  $\square$

## 8 Discussion and Conclusion

In light of recent work that has established that large informatics graphs such as social and information networks have non-trivial tree-like structure when viewed at moderate size scales, we have presented results from the first detailed empirical evaluation of the use of tree decomposition (TD) heuristics for structure identification and extraction in social graphs. Tree decompositions, and in particular the associated parameter of treewidth, provide a way to measure how tree-like a graph is in terms of its cut structure, and have been used extensively in both structural graph theory (from a theoretical perspective) and numerical linear algebra and scientific computing (from an applied heuristic perspective). After providing a detailed empirical evaluation of existing TD heuristics on toy and synthetic networks, we showed that these existing TD methods can identify interesting structure in a wide range of realistic informatics graphs. In light of our empirical and theoretical results, several areas are particularly ripe for further inquiry, and we conclude by briefly commenting on several of the most promising directions.

Clearly, there is a need to develop tree decomposition heuristics that are better-suited for the properties of realistic informatics graphs. This might involve making more sophisticated choices than greedily minimizing degree or fill, but it might also involve optimizing other parameters such as treelength (which has connections with  $\delta$ -hyperbolicity) or minimizing the width of bags that are not central (associated with the deep core). This is of interest not only for the social graph applications we have considered but also for many other application areas. In addition, it would be interesting to use TDs to help to combine small local clusters found with other methods, e.g., local spectral methods, into larger overlapping clusters, in order to understand better what might be termed the “local to global” properties of realistic informatics graphs. Since these graphs are not well-described by simple low-dimensional structures or simple constant-degree expander-like structures, this coupling is particularly counterintuitive, but it is very important for applications such as the diffusion of information. Finally, given the connections between TDs and graphical models, it would be interesting to understand better the implications of our results for improved graphical modeling and/or for improved inference on realistic network data. We expect that this will be a particularly challenging but promising direction for future work on social (as well as non-social) graphs.

**Acknowledgments.** We would like to thank Felix Reidl for considerable help in simplifying the proof of Theorem 3. We would also like to thank Mason Porter for helpful discussions and for providing several of the networks that we considered as well as Dima Krioukov and

his collaborators for providing us access to their code for generating networks based on their hyperbolic model. In addition, we would like to acknowledge financial support from the Air Force Office of Scientific Research, the Army Research Office, the Defense Advanced Research Projects Agency, the National Consortium for Data Science, and the National Science Foundation. Any opinions, findings, and conclusions or recommendations expressed in this publication are those of the author(s) and do not necessarily reflect the views of any of the above funding agencies.

## References

- [1] J. Leskovec, K.J. Lang, A. Dasgupta, and M.W. Mahoney. Community structure in large networks: Natural cluster sizes and the absence of large well-defined clusters. *Internet Mathematics*, 6(1):29–123, 2009. Also available at: arXiv:0810.1355.
- [2] L. G. S. Jeub, P. Balachandran, M. A. Porter, P. J. Mucha, and M. W. Mahoney. Think locally, act locally: The detection of small, medium-sized, and large communities in large networks. *Accepted for publication in: Physical Review E*. Also available at: arXiv:1403.3795.
- [3] A. B. Adcock, B. D. Sullivan, and M. W. Mahoney. Tree-like structure in large social and information networks. In *Proc. of the 2013 IEEE ICDM*, pages 1–10, 2013.
- [4] V. Batagelj and M. Zaversnik. Generalized cores. *CoRR*, cs.DS/0202039, 2002.
- [5] V. Batagelj and M. Zaversnik. An  $O(m)$  algorithm for cores decomposition of networks. *CoRR*, cs.DS/0310049, 2003.
- [6] V. Batagelj and M. Zaversnik. Fast algorithms for determining (generalized) core groups in social networks. *Advances in Data Analysis and Classification*, 5(2):129–145, 2011.
- [7] N. Robertson and P. D. Seymour. Graph minors. II. Algorithmic aspects of tree-width. *Journal of Algorithms*, 7(3):309–322, 1986.
- [8] S. Arnborg and A. Proskurowski. Linear time algorithms for NP-hard problems restricted to partial k-trees. *Discrete Applied Mathematics*, 23(1):11–24, 1989.
- [9] M. W. Bern, E. L. Lawler, and A. L. Wong. Linear-time computation of optimal subgraphs of decomposable graphs. *Journal of Algorithms*, 8(2):216–235, 1987.
- [10] A. M. C. A. Koster, S. P. M. van Hoesel, and A. W. J. Kolen. Solving partial constraint satisfaction problems with tree decomposition. *Networks*, pages 170–180, 2002.
- [11] J. Lagergren. Efficient parallel algorithms for graphs of bounded tree-width. *Journal of Algorithms*, 20(1):20–44, 1996.
- [12] I. V. Hicks, A. M. C. A. Koster, and E. Kolotoğlu. Branch and tree decomposition techniques for discrete optimization. *TutORials in Operation Research: INFORMS–New Orleans*, pages 1–29, 2005.
- [13] J. Zhao, R. L. Malmberg, and L. Cai. Rapid *ab initio* RNA folding including pseudoknots via graph tree decomposition. In *Proceedings of the 6th International Workshop on Algorithms in Bioinformatics*, pages 262–273, 2006.
- [14] J. Zhao, D. Che, and L. Cai. Comparative pathway annotation with protein-DNA interaction and operon information via graph tree decomposition. In *Pacific Symposium on Biocomputing*, pages 496–507, 2007.
- [15] C. Liu, Y. Song, B. Yan, Y. Xu, and L. Cai. Fast de novo peptide sequencing and spectral alignment via tree decomposition. In *Pacific Symposium on Biocomputing*, pages 255–266, 2006.
- [16] S. L. Lauritzen and D. J. Spiegelhalter. Local computations with probabilities on graphical structures and their application to expert systems (with discussion). *Journal of the Royal Statistical Society series B*, 50:157–224, 1988.

- [17] D. Karger and N. Srebro. Learning Markov networks: maximum bounded tree-width graphs. In *Proceedings of the 12th ACM-SIAM Symposium on Discrete algorithms*, pages 392–401, 2001.
- [18] H. Chen. Quantified constraint satisfaction and bounded treewidth. In *Proceedings of the 16th European Conference on Artificial Intelligence*, pages 161–165, 2004.
- [19] H. L. Bodlaender and R. H. Möhring. The pathwidth and treewidth of cographs. *SIAM Journal on Discrete Mathematics*, 6(2):181–188, 1993.
- [20] C. Chekuri and J. Chuzhoy. Polynomial bounds for the grid-minor theorem. *CoRR*, abs/1305.6577, 2013.
- [21] P.D. Seymour and R. Thomas. Call routing and the ratcatcher. *Combinatorica*, 14(2):217–241, 1994.
- [22] H. L. Bodlaender and A. M. C. A. Koster. Treewidth computations I. Upper bounds. *Inf. Comput.*, 208(3):259–275, 2010.
- [23] H. L. Bodlaender. A linear-time algorithm for finding tree-decompositions of small treewidth. *SIAM Journal on Computing*, 25(6):1305–1317, 1996.
- [24] E. Amir. Approximation algorithms for treewidth. *Algorithmica*, 56(4):448–479, 2010.
- [25] H. Röhrig. Tree decomposition: a feasibility study. Master’s thesis, Universität des Saarlandes, Saarbrücken, Germany, 1998.
- [26] K. Shokhet and D. Geiger. A practical algorithm for finding optimal triangulations. In *Proceedings of AAAI/IAAI*, pages 185–190, 1997.
- [27] C. Groér, B. D. Sullivan, and D. Weerapurage. INDDGO: Integrated network decomposition & dynamic programming for graph optimization. Technical Report ORNL/TM-2012/176, Oak Ridge National Laboratory, 2012.
- [28] B. D. Sullivan et al. Integrated Network Decompositions and Dynamic programming for Graph Optimization (INDDGO), 2012, 2013. <http://github.com/bdsullivan/inddgo>.
- [29] F. Gavril. The intersection graphs of subtrees in trees are exactly the chordal graphs. *Journal of Combinatorial Theory, Series B*, 16(1):47–56, 1974.
- [30] D. J. Rose and R. E. Tarjan. Algorithmic aspects of vertex elimination. In *Proceedings of the 7th Annual ACM Symposium on Theory of Computing*, pages 245–254, 1975.
- [31] A. Berry, J. R. S. Blair, and P. Heggernes. Maximum cardinality search for computing minimal triangulations. In *Proceeding of the 28th International Workshop on Graph-Theoretic Concepts in Computer Science*, pages 1–12, 2002.
- [32] A. Berry, J. R. S. Blair, P. Heggernes, and B. W. Peyton. Maximum cardinality search for computing minimal triangulations of graphs. *Algorithmica*, 39(4):287–298, 2004.
- [33] D. Rose, R. Tarjan, and G. Lueker. Algorithmic aspects of vertex elimination on graphs. *SIAM Journal on Computing*, 5:266–283, 1976.
- [34] R. E. Tarjan and M. Yannakakis. Simple linear-time algorithms to test chordality of graphs, test acyclicity of hypergraphs, and selectively reduce acyclic hypergraphs. *SIAM Journal on Computing*, 13:566–579, 1984.
- [35] R. E. Tarjan and M. Yannakakis. Addendum: Simple linear-time algorithms to test chordality of graphs, test acyclicity of hypergraphs, and selectively reduce acyclic hypergraphs. *SIAM Journal on Computing*, 14(1):254–255, 1985.
- [36] A. Becker and D. Geiger. A sufficiently fast algorithm for finding close to optimal clique trees. *Artificial Intelligence*, 125(1–2):3–17, 2001.
- [37] H. L. Bodlaender, J. R. Gilbert, H. Hafsteinsson, and T. Kloks. Approximating treewidth, pathwidth, and minimum elimination tree height. *Journal of Algorithms*, 18:238–255, 1995.

- [38] V. Bouchitté, D. Kratsch, H. Müller, and I. Todinca. On treewidth approximations. *Discrete Appl. Math.*, 136(2-3):183–196, 2004.
- [39] B. A. Reed. Finding approximate separators and computing tree width quickly. In *Proceedings of the 24th Annual ACM Symposium on Theory of Computing*, pages 221–228, 1992.
- [40] J. A. George. Nested dissection of a regular finite element mesh. *SIAM Journal of Numerical Analysis*, 10:345–363, 1973.
- [41] J. R. Gilbert and R. E. Tarjan. The analysis of a nested dissection algorithm. *Numerische Mathematik*, 50(4):377–404, 1986.
- [42] G. Karypis and V. Kumar. A fast and high quality multilevel scheme for partitioning irregular graphs. *SIAM Journal on Scientific Computing*, 20(1):359–392, 1998.
- [43] H. M. Markowitz. The elimination form of the inverse and its application to linear programming. *Management Science*, 3(3):255–269, 1957.
- [44] P. R. Amestoy, T. A. Davis, and I. S. Duff. Algorithm 837: AMD, an approximate minimum degree ordering algorithm. *ACM Transactions on Mathematical Software (TOMS)*, 30(3):381–388, 2004.
- [45] P. R. Amestoy, T. A. Davis, and I. S. Duff. An approximate minimum degree ordering algorithm. *SIAM Journal on Matrix Analysis and Applications*, 17(4):886–905, 1996.
- [46] D. Koller and N. Friedman. *Probabilistic Graphical Models: Principles and Techniques*. MIT Press, 2009.
- [47] H. L. Bodlaender. A tourist guide through treewidth. *Acta Cybernetica*, 11:1–23, 1993.
- [48] H. L. Bodlaender. Discovering treewidth. In *Proceedings of the 31st international conference on Theory and Practice of Computer Science*, pages 1–16, 2005.
- [49] H. L. Bodlaender. Treewidth: Characterizations, applications, and computations. In *Proceeding of the 32nd International Workshop on Graph-Theoretic Concepts in Computer Science*, pages 1–14, 2006.
- [50] H. L. Bodlaender and A. M. C. A. Koster. Combinatorial optimization on graphs of bounded treewidth. *The Computer Journal*, 51(3):255–269, 2007.
- [51] J. R. S. Blair and B. Peyton. An introduction to chordal graphs and clique trees. In A. George, J. R. Gilbert, and J. W. H. Liu, editors, *Graph Theory and Sparse Matrix Computation*, The IMA Volumes in Mathematics and its Applications, Volume 56, pages 1–29. Springer-Verlag, 1993.
- [52] E. Amir. Efficient approximation for triangulation of minimum treewidth. In *Proceedings of the 17th Annual Conference on Uncertainty in Artificial Intelligence*, pages 7–15, 2001.
- [53] A. M. C. A. Koster, H. L. Bodlaender, and S. P. M. van Hoesel. Treewidth: Computational experiments. *Electronic Notes in Discrete Mathematics*, 8:54–57, 2001.
- [54] A. Berry, P. Heggernes, and G. Simonet. The minimum degree heuristic and the minimal triangulation process. In *Proceeding of the 29th International Workshop on Graph-Theoretic Concepts in Computer Science*, pages 58–70, 2003.
- [55] P. Heggernes. Minimal triangulations of graphs: A survey. *Discrete Mathematics*, 306(3):297–317, 2006.
- [56] C. Wang, T. Liu, P. Cui, and K. Xu. A note on treewidth in random graphs. In *Proceeding of the 5th International Conference on Combinatorial Optimization and Applications*, pages 491–499, 2011.
- [57] Y. Gao. Treewidth of Erdős-Rényi random graphs, random intersection graphs, and scale-free random graphs. *Discrete Applied Mathematics*, 160(4–5):566–578, 2012.
- [58] M. Gromov. Hyperbolic groups. In S. M. Gersten, editor, *Essays in Group Theory*, Math. Sci. Res. Inst. Publ., 8, pages 75–263. Springer, 1987.

- [59] J. M. Alonso, T. Brady, D. Cooper, V. Ferlini, M. Lustig, M. Mihalik, H. Shapiro, and H. Short. Notes on word hyperbolic groups. In E. Ghys, A. Haefliger, and A. Verjovski, editors, *Group Theory from a Geometrical Viewpoint, ICTP Trieste Italy*, pages 3–63. World Scientific, 1991.
- [60] E. A. Jonckheere, P. Lohsoonthorn, and F. Bonahon. Scaled Gromov hyperbolic graphs. *Journal of Graph Theory*, 57(2):157–180, 2008.
- [61] E. A. Jonckheere, P. Lohsoonthorn, and F. Ariaei. Scaled Gromov four-point condition for network graph curvature computation. *Internet Mathematics*, 7(3):137–177, 2011.
- [62] W. Chen, W. Fang, G. Hu, and M. W. Mahoney. On the hyperbolicity of small-world and tree-like random graphs. *Internet Mathematics*, 9(4):434–491, 2013. Also available at: arXiv:1201.1717.
- [63] A. B. Adcock, B. D. Sullivan, O. R. Hernandez, and M. W. Mahoney. Evaluating OpenMP tasking at scale for the computation of graph hyperbolicity. In *Proc. of the 9th IWOMP*, pages 71–83, 2013.
- [64] K. Verbeek and S. Suri. Metric embedding, hyperbolic space, and social networks. In *Proceedings of the 30th Annual Symposium on Computational Geometry*, pages 501–510, 2014.
- [65] G. Brinkmann, J. H. Koolen, and V. Moulton. On the hyperbolicity of chordal graphs. *Annals of Combinatorics*, 5(1):61–69, 2001.
- [66] Y. Wu and C. Zhang. Hyperbolicity and chordality of a graph. *The Electronic Journal of Combinatorics*, 18(1):P43, 2011.
- [67] Y. Dourisboure and C. Gavoille. Tree-decompositions with bags of small diameter. *Discrete Mathematics*, 307(16):2008–2029, 2007.
- [68] D. Lokshtanov. On the complexity of computing treelength. In *Proceedings of the 32nd international conference on Mathematical Foundations of Computer Science*, pages 276–287, 2007.
- [69] M. Grohe and D. Marx. On tree width, bramble size, and expansion. *Journal of Combinatorial Theory Series B*, 99(1):218–228, 2009.
- [70] A. Kosowski, B. Li, N. Nisse, and K. Suchan.  $k$ -chordal graphs: From cops and robber to compact routing via treewidth. In *Proceedings of the 39th international colloquium conference on Automata, Languages, and Programming*, pages 610–622, 2012.
- [71] F. F. Dragan. Tree-like structures in graphs: A metric point of view. In *Proceeding of the 39th International Workshop on Graph-Theoretic Concepts in Computer Science*, pages 1–4, 2013.
- [72] M. Abu-Ata and F. F. Dragan. Metric tree-like structures in real-life networks: an empirical study. *CoRR*, abs/1402.3364, 2014.
- [73] M. M. Abu-Ata. *Tree-Like Structure in Graphs and Embeddability to Trees*. PhD thesis, Kent State University, 2014.
- [74] Y. Shavitt and T. Tankel. Hyperbolic embedding of internet graph for distance estimation and overlay construction. *IEEE/ACM Transactions on Networking*, 16(1):25–36, 2008.
- [75] M. P. Rombach, M. A. Porter, J. H. Fowler, and P. J. Mucha. Core-periphery structure in networks. *CoRR*, abs/1202.2684, 2012.
- [76] S. B. Seidman. Network structure and minimum degree. *Social Networks*, 5(3):269–287, 1983.
- [77] J. Ignacio Alvarez-Hamelin, L. Dall’Asta, A. Barrat, and A. Vespignani. Large scale networks fingerprinting and visualization using the k-core decomposition. In *Annual Advances in Neural Information Processing Systems 18: Proceedings of the 2005 Conference*, pages 41–50, 2006.
- [78] J. Ignacio Alvarez-Hamelin, L. Dall’Asta, A. Barrat, and A. Vespignani. K-core decomposition of Internet graphs: hierarchies, self-similarity and measurement biases. *Networks and Heterogeneous Media*, 3(2):371–293, 2008.
- [79] J. Healy, J. Janssen, E. Milios, and W. Aiello. Characterization of graphs using degree cores. In *WAW ’08: Proceedings of the 6th Workshop on Algorithms and Models for the Web-Graph*, pages 137–148, 2008.

- [80] V. Batagelj and A. Mrvar. Pajek - analysis and visualization of large networks. In *Graph Drawing Software*, pages 77–103, 2003.
- [81] J. Cheng, Y. Ke, S. Chu, and M. T. Ozsu. Efficient core decomposition in massive networks. In *Proceedings of the 27th IEEE International Conference on Data Engineering*, pages 51–62, 2011.
- [82] P. Colomer-de Simon, A. Serrano, M. G. Beiro, J. Ignacio Alvarez-Hamelin, and M. Boguna. Deciphering the global organization of clustering in real complex networks. *CoRR*, abs/1306.0112, 2013.
- [83] M. Kitsak, L. K. Gallos, S. Havlin, F. Liljeros, L. Muchnik, H. E. Stanley, and H. A. Makse. Identification of influential spreaders in complex networks. *Nature Physics*, 6:888–893, 2010.
- [84] J. Ugander, L. Backstrom, C. Marlow, and J. Kleinberg. Structural diversity in social contagion. *Proceedings of the National Academy of Sciences*, 109(16):5962–5966, 2012.
- [85] V. Ramasubramanian, D. Malkhi, F. Kuhn, M. Balakrishnan, A. Gupta, and A. Akella. On the treeness of internet latency and bandwidth. In *Proceedings of the 2009 ACM SIGMETRICS International Conference on Measurement and modeling of computer systems*, pages 61–72, 2009.
- [86] F. de Montgolfier, M. Soto, and L. Viennot. Treewidth and hyperbolicity of the internet. In *Proceedings of the 10th IEEE International Symposium on Network Computing and Applications (NCA)*, pages 25–32, 2011.
- [87] T. Maehara, T. Akiba, Y. Iwata, and K. Kawarabayashi. Computing personalized PageRank quickly by exploiting graph structures. *Proceedings of the VLDB Endowment*, 7:1023–1034, 2014.
- [88] A. G. Percus, G. Istrate, B. Goncalves, R. Z. Sumi, and S. Boettcher. The peculiar phase structure of random graph bisection. *Journal of Mathematical Physics*, 49(12):125219, 2008.
- [89] F.R.K. Chung and L. Lu. *Complex Graphs and Networks*, volume 107 of *CBMS Regional Conference Series in Mathematics*. American Mathematical Society, 2006.
- [90] Supporting website. <http://snap.stanford.edu/data/index.html>.
- [91] A. L. Traud, P. J. Mucha, and M. A. Porter. Social structure of Facebook networks. *CoRR*, abs/1102.2166, 2011.
- [92] L. A. Adamic and N. Glance. The political blogosphere and the 2004 U.S. election: divided they blog. In *Proceedings of the 3rd international workshop on Link discovery*, pages 36–43, 2005.
- [93] D. J. Watts and S. H. Strogatz. Collective dynamics of small-world networks. *Nature*, 393:440–442, 1998.
- [94] E. R. Gansner and S. C. North. An open graph visualization system and its applications to software engineering. *SoftwarePractice and Experience*, 30(11):1203–1233, 2000.
- [95] T. A. Davis and Y. Hu. The University of Florida Sparse Matrix Collection. *ACM Transactions on Mathematical Software (TOMS)*, 38(1):1:1–1:25, 2011.
- [96] T. Malisiewicz. Open source code: Graphviz matlab magic. [https://github.com/quantombone/graphviz\\_matlab\\_magic](https://github.com/quantombone/graphviz_matlab_magic), May 2010.
- [97] P. Erdős and A. Rényi. On the evolution of random graphs. *Publ. Math. Inst. Hungar. Acad. Sci.*, 5:17–61, 1960.
- [98] B. Bollobás. *Random Graphs*. Academic Press, London, 1985.
- [99] R. Andersen, F.R.K. Chung, and K. Lang. Local graph partitioning using PageRank vectors. In *FOCS '06: Proceedings of the 47th Annual IEEE Symposium on Foundations of Computer Science*, pages 475–486, 2006.
- [100] M. Müller. Connected tree-width. *CoRR*, abs/1211.7353, 2012.
- [101] V. Chepoi, F. Dragan, B. Estellon, M. Habib, and Y. Vaxès. Diameters, centers, and approximating trees of  $\delta$ -hyperbolic geodesic spaces and graphs. In *Proceedings of the 24th Annual Symposium on Computational Geometry*, pages 59–68, 2008.

- [102] P. Bellenbaum and R. Diestel. Two short proofs concerning tree-decompositions. *Combinatorics, Probability, and Computing*, 11:541–547, 2002.